

# Review of Experimental and Finite Element Analyses of Spot Weld Failures in Automotive Metal Joints

Aravinthan Arumugam\*, Alokesh Pramanik

*School of Civil and Mechanical Engineering, Curtin University, Kent.St, WA 6102, Australia*

*Received April 25 2020*

*Accepted August 30 2020*

## Abstract

The spot weld failure analysis using experimental and numerical finite element analysis methods has been reviewed. The spot weld strength is governed by the welding parameters, sheet metal thicknesses and the loading conditions. Spot weld fails either by pull-out failure (PF) mode or interfacial failure (IF) mode. The spot weld failure modes depend on the diameter of weld and the loading types. Most reported experimental spot weld failure analyses were based on industrial standard test samples under quasi static loading. Limited work on combined loading on dissimilar metal joints with different thicknesses was found in the review. The review further observed that weld bonded joints have better fatigue life compared to spot welded joints. Extensive work has been proposed in this review on this type of hybrid joints as current research showed limited investigation in this area. In the finite element analysis of spot weld failures, current researches mostly investigated single spot weld failures using the standard tests under quasi static loading. The review proposed further study of spot weld failure of multiple spot welds under fatigue loading for dissimilar joints and hybrid joints. Finally, a hybrid system has been proposed to relate the experimental and computational weld failure analyses for spot weld optimization.

© 2020 Jordan Journal of Mechanical and Industrial Engineering. All rights reserved

*Keywords: spot weld; failure mode; diameter; strength; weld joint; lap-shear; coach -peel; cross-tension; FEA; quasi-static; fatigue;*

## 1. Introduction

The typical joining method used for joining automotive metals together is the welding process. Different types of welding processes have been employed in the automotive manufacturing, such as resistance spot welding (RSW), resistance seam welding (RSEW), friction welding (FW), laser beam welding (LBW) and arc welding. However, the welding process that is widely used in the Body in White (BIW) fabrication and still dominates the automotive industry is the resistance spot welding (RSW). Popularly known as the spot welding, the welding process gained its popularity because of being a cost-effective process, easily automated, and has a rapid production rate, low component distortion as well as its simplicity and versatility. Automotive BIW has about 2000-5000 spot welds used to join the different types and shapes of metal sheets together. Numerous studies have been carried out in the use of the spot-welding process to join similar and dissimilar metals, such as Advanced High-Speed Steels (AHSS), aluminium and magnesium, a design strategy known as multi-materials lightweight (MML) design.<sup>[1-7]</sup> With a large number of spot welds involved in the forming of automotive BIW, the spot welding process has close relationship with the structural integrity and performance of the BIW. The spot welds function as the elements responsible in load bearing and load transfer during automotive crash and impact. The

strength of the individual spot weld plays a role in ensuring that it can sustain the impact load without failing and maintaining the structural strength of the BIW while providing safety of passengers.

However, as the trend of automotive metals is going towards lighter metals yet stronger metals with lesser thicknesses, the control of the spot weld strength has become a challenge for the automotive manufacturers. The strength of a spot weld depends on various factors, such as material weldability, sheet thickness, spot weld positions, welding parameters, material coating, joint and loading types.<sup>[8-13]</sup> Due to the inherent uncertainty on an individual spot weld's strength, automotive industries tend to add significant number of redundant spot welds to ensure the structural integrity of the BIW is achieved.<sup>[14]</sup> These redundant spot welds obviously increase the overall spot weld manufacturing cost and could be eliminated if the spot weld failures under different loading conditions can be predicted earlier during design stage. The optimization of the number of spot welds and the positions for spot welds are crucial in reducing the RSW related manufacturing cost. With the advancement in computer technology and the field of finite element analysis (FEA), such prediction is now possible.

There are numerous researches in this area and many results are reported. However, those are not well organised and properly linked. In fact, it is not easy to have a complete understanding in this area though it is essential for

\* Corresponding author e-mail: aravinthan.arumugam@curtin.edu.au

improving the efficiency and effectiveness of spot-welding testing. To address this issue, this paper critically reviews and scientifically links the information available in the recent works related to spot weld failure on different automotive metals, the spot weld failure modes as a result of different loading conditions and finally the use of experimental and numerical FEA in spot weld failure analysis and prediction. The paper also aims to propose future work in the area of experimental and computational spot weld failure analyses and development of a hybrid system for failure analyses.

## 2. Spot welding

The spot-welding process consists of two water cooled copper electrodes, connected electrically to a welding transformer. The electrodes are usually actuated through an upwards and downward motion by means of pneumatic or servo motor-based actuation system. The metal sheets to be welded are placed in between the copper electrodes and the area to be welded is brought into intimate contact by the force applied by the clamped electrodes during squeeze cycle. In the weld cycle, the welding current is then supplied through the upper electrode which flows to the lower electrode through the metal sheets and the sheet interface. As the resistance to current flow is greater at the sheets interface compared to the bulk material of the sheet metals, the copper electrodes and the electrode and sheet interface, localised heating and melting will occur at the sheets interface. The melting area is related to the diameter of both the copper electrodes which are compressing the metal sheets together. After a pre-set weld time, during hold cycle, the current is turned off, but the electrode force is maintained while the weld solidifies and joins both metal sheets together via a spot weld. Figure 1 gives the schematic of the spot-welding process.

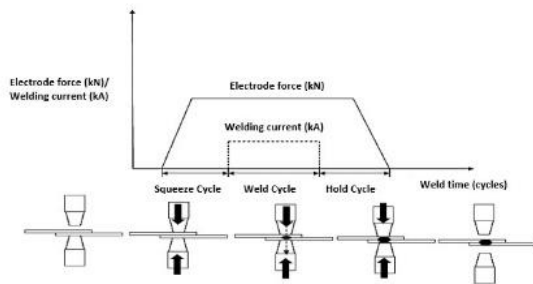


Figure 1. Spot welding process

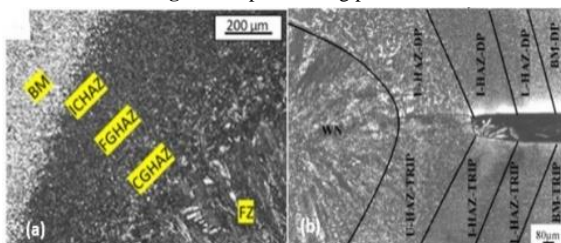


Figure 2. Microstructural zones in (a) Galvannealed DP600/bare DP600<sup>[42]</sup> and (b) DP1000/TRIP 980<sup>[43]</sup> weld joints

The heat generated during the spot-welding process can be represented by the Equation (1)

$$Q = \int_{T_1}^{T_2} I(t)^2 R(t) dt \quad (1)$$

where the  $Q$  is the heat generated during the welding process,  $I(t)$  is the supplied current,  $R(t)$  is the dynamic resistance of the sheet metals,  $T_1$  and  $T_2$  are the time limits of the process respectively.

## 3. Welding parameters and weld strength

The spot-welding process mainly has three important parameters based on the Equation 1, which controls the heat generation during welding for spot weld formation and directly impacts the weld strength. The process parameters are weld current, electrode force and weld time. Increase in the spot weld current with weld time and electrode force maintained constant or the increase in weld time with both welding current and electrode force maintained constant during the welding of two metal sheets, has been reported to increase the heat generation during spot welding process. The increased heat generation in turn increased the size of the spot weld diameter as well as the weld strength.[10, 15-21] Taguchi method has been used by various authors to analyse the contribution of both the welding current and weld time in the heat generation for spot weld formation. Welding current has been shown to have major contribution in heat generation and spot weld development during the welding process with ANOVA results giving an average of 60.9% for welding current and 20.6% for weld time. [15, 18, 22-25] However, the increase in welding current and weld time are limited to a certain range, after which further increase in either parameter, will cause expulsion during welding. Expulsion is referred to as the ejection of molten metal from the weld zone due to overheating. Presence of expulsion was found to cause excessive electrode indentation, shrinkage void and solidification cracks in spot weld, leading to deterioration of spot weld strength. Expulsion was found to occur at the electrode/sheet metal interface and sheet metal/sheet metal interface. [26, 27]

The third weld parameter, that contributes to the heat generation in the welding process and relates closely to the dynamic resistance in Equation 1 is the electrode force.[28] Unlike welding current and weld time, decreasing electrode force while maintaining welding current and weld time, increased the heat generation during spot welding process. Lower electrode force will increase the resistance to current flow at the sheets' interface due to high number of surface asperities and lower sheet-to-sheet surface contact. This leads to increase in the current density and in turn increase the heat generation at the interface for weld development. Higher electrode force will cause these surface asperities to collapse creating increased sheet-to-sheet surface contact. Current density will therefore decrease leading to reduction in heat generation. However, extremely low electrode force will cause expulsion mainly due to overheating and very high electrode force will lead to development of undersized weld due to low heat generation.[29, 30]

Traditionally, welding current has been the only control parameter in spot welding to control the development of spot weld and in turn the achieved weld strength. Welding current was easy to measure with the use of current probes or transducers and the amperage that is supplied to the weld joint can be controlled by controlling the individual firing angles of the two silicon-controlled rectifiers (SCRs) in a single-phase AC resistance spot welding machine. The

control strategy which is known as the constant current control (CCC) has been discussed by Zhou.[31, 32] As most of these welding machines were based on pneumatically actuated electrode system, force was not used as a control parameter due to the inability to control the electrode force at a faster rate with the use of the mechanical system. This is due to the inherent mechanical inertia in the pneumatic system. However, when the electronically controlled electrodes by servo drives were introduced, this created an opportunity for electrode force to be included as a control parameter apart from welding current. The advantages of servo actuated electrodes are that the electrodes' position, speed and applied force (electrode force) can be precisely controlled.[33] As spot welding process is naturally a non-linear process involving different variables (current, time, electrode force, sheet thickness, electrode diameter, mechanical and electrical characteristics of machine used etc) and interaction between electrical, thermal, mechanical and metallurgical changes at the sheets interface, the application of more than one control parameter to control the weld nugget development and weld strength was widely investigated. Also, with the automotive industries increasingly use different types of sheet metals with various thickness to fabricate the BIW, in-process real time control of welding parameters was studied to achieve stringent quality control of spot welds. The use of force and current profiles i.e step control of welding current and servo system driven electrode force to control both parameters in real-time during welding and the improvements that were achieved in terms of the weld strength, expulsion reduction and ability to weld joints with different materials and thicknesses have been reported by different studies. [34-38]

Even though weld current, time and electrode force are the basic parameters in the spot-welding process to produce spot welds, the melting of metal at the sheets interface and development of weld nugget is influenced by the dynamic contact resistance. The dynamic contact resistance accounts for the combined effect of the interfacial resistance and bulk material resistance.[39] Shome and Chatterjee[39] concluded from their study that dynamic contact resistance which determines the energy input and control spot weld formation is dependent on the coating type, thickness, surface roughness, bulk material resistance and external factors, such as temperature and pressure. From the previous factors, thickness and bulk material resistance relate closely to the problem that is faced by the automotive industries, joining dissimilar materials. Automotive structure design involves dissimilar metals with different thicknesses. Formation of a sound spot weld between two different metals requires an efficient heat balance in both metals considering the different material properties of the metals. This results in the formation of a weld nugget of approximately the same thickness on each side of the sheets interface.[40] Numerous works have been researched in the weldability of materials of dissimilar metals to form spot weld joint.

The weldability and failure of spot weld between two dual phase steels; DP600 and DP1000 with 0.8 mm thickness and galvanized and bare DP600 with 1.3 mm thickness were studied by Aydin[41] and Kishore et al.[42] respectively. Weld nugget size and weld strength were found to increase by increase in welding current. These studies also found that weld formed by both the DP steels

has three distinct microstructural zones; base metal (BM), fusion zone (FZ) and heat affected zone (HAZ). In the heat affected zones, there are further transition zones; outer heat affected zone (OHAZ), centre heat affected zone (CHAZ) and inner heat affected zone (IHAZ)[41] or inter critical heat affected zone (ICHAZ), fine grain heat affected zone (FGHAZ) and coarse grain in heat affected zone (CCHAZ).[42] As for failure mode, pull out failure was obtained for the range of current investigated. From the lowest current to the intermediate current, failure occurred at the CHAZ on the DP1000 side and above the intermediate current till the highest current, failure occurred at the CHAZ on the DP600 side.[41] Mousavi et al.[16] studied the optimization of process parameters to join dissimilar metals; DP600 and AISI304 stainless steel with thickness of 1 mm. The study revealed that the microstructure of the DP steel's HAZ is martensitic and the AISI304 steel's HAZ is austenitic. Also, the microstructure of the FZ is fully martensitic with the FZ chemical composition influenced by the chemical compositions of both the AISI304 steel and DP steel. Weld failure test carried out with tensile lap-shear test also showed at optimum parameters, weld pull-out failure is obtained with the failure occurring at the AISI304 stainless BM. The weldability of similar and dissimilar joints between 1.36 mm thick DP1000 steel and 1.56 mm thick transformation induced plasticity (TRIP980) steel was studied by Wei et al.[43] Similar to Aydin and Kishore's work[41, 42], the microstructural study between DP/DP, TRIP/TRIP and DP/TRIP showed three distinct microstructural zones; base metal (BM), fusion zone (FZ) and heat affected zone (HAZ). For the DP/TRIP weld joint, the heat affected zone is further divided into; upper heat affected zone (UHAZ), intermediate heat affected zone (IHAZ) and lower heat affected zone (LHAZ). The weld nugget diameter and weld strength for similar joints (DP/DP and TRIP/TRIP) and dissimilar joints (DP/TRIP) increased with increase in current till a certain current limit after which due to expulsion both properties of the spot weld reduced at higher current. The study also showed the FZ of all joints exhibit fully martensite microstructure and the spot weld failure in pull out mode increased in the order of DP/DP, TRIP/TRIP and DP/TRIP. Figures 2(a) and 2(b) show the different microstructural zones in the galvanized and bare DP600 and DP1000/TRIP980

Liu et al.[44] studied the weldability of similar and dissimilar spot welds made from lightweight magnesium alloy (Mg) and high strength low alloy (HSLA) steel. The thickness of Mg strip is 1.5 mm and the HSLA steel thickness is 0.77 mm. Interestingly unlike in Mg/Mg joint, in Mg/steel joint, FZ representing weld nugget, was only noticed on the Mg side while Mg and steel was bonded by three different regions; weld brazing, solid-state joining and soldering as in Figure 3. The hardness test on the Mg/steel joint showed that the hardness on the steel side of the joint is almost twice the hardness of the Mg side. As for weld failure in this study, fatigue test was carried out and the test showed initiation of crack at the Mg/steel interface. The crack propagates further at higher rate into the Mg base metal until failure occurred. However, at the steel side, a slower crack propagation rate was noticed along the Mg and steel interface into the weld nugget. Manladan et al.[45] studied the spot welding of Mg alloy and austenitic stainless steel under two joints; dissimilar spot welded joint (RSW)

and dissimilar spot weld-bonded joint (RSWB) using epoxy structural adhesive. Lap-shear test was carried out to analyse weld failure on these joints. The results showed that for a range of welding currents (6 kA to 18 kA), RSWB joints have higher bonding diameters, peak loads and energy absorption prior to failure compared to RSW joints. The failure analysis observed that in RSW spot weld failure, failure occurred through the Mg nugget/stainless steel interface and weld zone formed through welding brazing mode as reported by Liu[44].

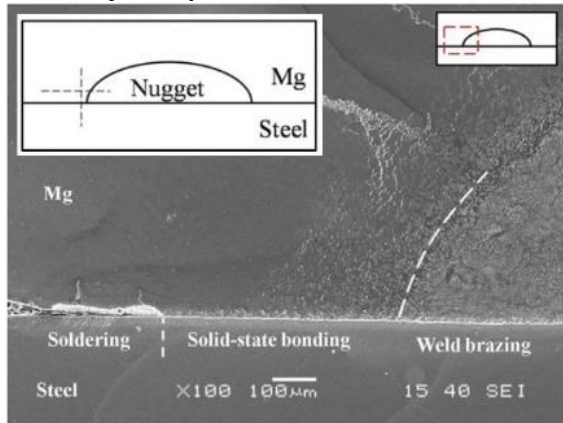


Figure 3. Microstructure of Mg/HSLA weld joint<sup>[44]</sup>

The weldability of aluminium alloy with steel was investigated by Miyamoto et al.[46] The study investigated joining of steel with aluminium alloy; galvanized steel (GA) with 600 series aluminium alloy (Al) plate with 0.55 mm and 1 mm thicknesses respectively. The GA are coated by layer of FeZn8 ( $\delta$  phase). Two types of samples were created; resistance spot welded sample by welding both metals together and seal spot welded sample by having a sealant in between both metals. For both samples, nugget diameter was found to increase with increase in time with welding current maintained at 30 kA for resistance spot weld sample and 27.5 kA for seal spot weld sample. The nugget diameter in the steel side and the formation of Al-Fe intermetallic compound (IMC) layer at the joint interface is shown in Figure 4[5]. The study also reported that seal spot welded joints can inhibit electrolytic corrosion while electrolytic corrosion occurred at the joint interface of resistance spot welded joint. To analyse the weld strength, cross tension test was carried out. Weld pull-out failures were observed for both samples with failure occurring at the aluminium alloy and the circular spot weld remaining on the steel. The decrease in aluminium sheet thickness during welding was deduced as the reason for failure on the aluminium sheet. Strength comparison between resistance spot welded joint and seal spot welded joint also showed that for the same welding condition, cross tension strength of seal spot weld joints is approximately half that of the resistance spot welded joints. The difference in strength between samples was related to the difference between the degrees of decrease in the sheet thickness of the aluminium alloy in the resistance spot weld joints and seal spot weld joints. The reduction in sheet thickness in the Al side and its influence to weld strength have also been reported by Sakiyama et al.[47].

The weldability of spot weld joints of AA5052 aluminium alloy with dissimilar thickness was investigated by Mat Din et al.[48] One sheet had a constant thickness of

2 mm and the other sheet thickness was varied from 1.2 to 3.2 mm (7 different sheet thicknesses). Peel test was carried out to analyse the spot weld failure due to different thicknesses. Increasing the sheet thickness increased nugget diameter and weld time. Failure strength to achieve pull out failure also initially increased till thickness combination of 2 mm - 2.3 mm after which there was a drop in strength till the last combination of 2 mm - 3.2 mm. Hence from the reviews in this section, it can be concluded that in order to obtain spot welds with strengths required to maintain the structural integrity of the of the automotive structure. Attention must be focused on the welding current and electrode force used during spot welding. The correct combination of welding current and electrode will generate the heat required for spot weld nugget initiation and development. Also, another important consideration is due to the increase use of dissimilar metal and sheet thicknesses in automotive structures, fundamental knowledge in metallurgical transformation in dissimilar metals and heat balance for both dissimilar metals and dissimilar thicknesses are required for welding parameters selection to produce spot welds that are well developed on both the metal sheets creating a strong joint at the sheets interface.

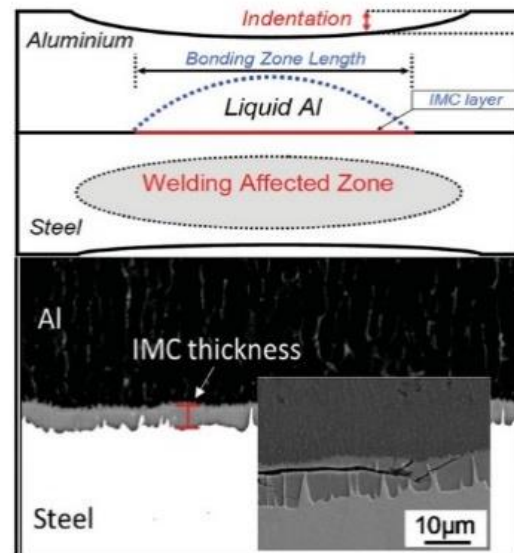
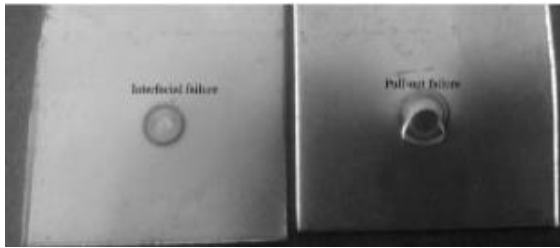


Figure 4. The microstructure in the Al/steel joint with the IMC layer at sheets interface<sup>[5]</sup>

#### 4. Experimental weld failure analysis

As seen in previous section, spot weld strength is influenced by the selection of the welding parameters as well as the metallurgical transformation and heat balance in the sheets to be welded. Weld failure modes are of two types; pull-out failure (PF) (failure due to weld pulled out from one sheet) and interfacial failure (IF) (failure due to crack propagation through the fusion zone) as seen in Figure 5. [49-51] Other authors have also further divided the failure modes into an intermediate failure mode called the partial interfacial failure (PIF) or partial pull-out failure (PPF).[49, 52, 53] Automotive industries require spot welds to fail by pull-out failure mode rather than interfacial failure mode as the former has higher failure load and absorb more energy prior to failure compared to the latter.[54]



**Figure 5.** Interfacial failure (IF) and pull out failure (PF) of spot weld joints

The weld diameter and loading conditions influence the tendency of the spot weld to fail by either failure modes. Spot welds fail by PF mode above the critical weld diameter and IF mode below the critical diameter.[55, 56] Critical diameter is defined as the minimum weld diameter required to achieve pull-out failure. Abadi[57] has also defined critical weld diameter as the weld diameter between the maximum weld diameter which will produce IF mode and the minimum weld diameter which will produce the PF mode. Pouranvari[56] developed a relationship to calculate the critical diameter ( $d_{cr}$ ) based on the relationship between the ultimate tensile stress of pull-out failure location ( $\sigma_{UTS}FL$ ) and the shear strength at the fusion zone ( $\tau_{FZ}$ ) as given in Equation (2).

$$d_{cr} = 4t \frac{(\sigma_{UTS})_{FL}}{\tau_{FZ}} \tag{2}$$

Similarly Zhao et.al[58] suggested Equation (3) as the critical nugget diameter to achieve PF mode for DP600 joints. This relationship was also developed considering the tensile stress at the HAZ and shear stress at FZ.

$$d_{cr} = 3.51t \tag{3}$$

where  $t$  is the sheet thickness in mm for both equations.

These equations are, however, based on the lap-shear test which will be discussed later. The standard used by the automotive industries states that to achieve PF mode, the average weld diameter is equal to  $4\sqrt{t}$  where,  $t$  is the sheet thickness[49]. This standard is, however, based on tensile-shear static loading to produce spot weld failure. Spot welds in real conditions for instance in automotive crashes, experience mixed loading such as shear force ( $f_s$ ), normal force ( $f_n$ ), bending moment ( $m_b$ ) and in-plane torsion ( $m_t$ ) as shown on Figure 6.[59]

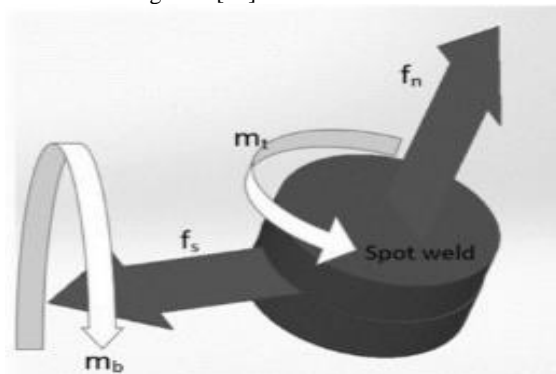


**Figure 6.** Loadings on spot weld

Failure of spot welds are due to two loading conditions; quasi static loading i.e load is applied slowly with low strain rate to deform a structure with inertia effects neglected and dynamic loading i.e will cause the structure to vibrate and the inertia force needs to be considered. Spot weld performance is based on its static and dynamic strength.[60] Hence it is important for the automotive design engineers to understand the mechanical behaviours of joints subjected to both static and dynamic loading conditions and incorporate the static strength, impact and fatigue strength in the early design stage. As a single, standard experiment is not available to evaluate the effect of all the forces to spot weld failure modes, experimental analyses have used three different test samples to separately analyse spot weld failure due to shear force, normal force and bending moment. The test samples are as shown in Figure 7. Test sample A is used to analyse spot weld failure due to bending moment and the test is named as the coach peel test. Test samples B and C are used in lap-shear and KSII tests, respectively. Sample B is used to evaluate the tensile and shear load on spot weld and sample C is used to test the normal load (90o) that will fracture the spot weld.

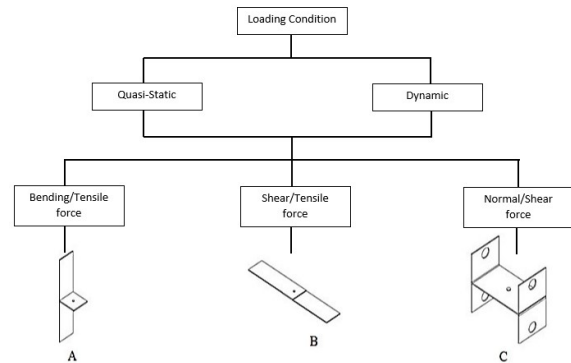


**Figure 7.** Spot weld loading conditions and test samples

Various works have been reported on the test samples used to analyse spot weld failures. Lap-shear test is the common test that has been widely used by many researchers in their spot weld failure experiments. Pouranvari[56] analysed weld failure with lap shear test for weld joints made from high strength low alloy (HSLA) 420 steel. The study showed the relationship between welding current, weld diameter or fusion zone size and the interfacial and pull-out failure modes as shown in Figure 8. The study reported that the driving force for IF mode in lap shear test is the shear stress at the sheet/sheet interface. Meanwhile the driving force for PF mode is the tensile stress at the nugget circumference. An equation was also suggested as in Equation (3) to calculate the PF load in tensile shear test.

$$PPF = \pi dt(\sigma_{UTS})_{FL} \tag{3}$$

where  $d$ - weld diameter,  $t$  – sheet thickness and  $(\sigma_{UTS})_{FL}$  – ultimate tensile strength at failure location which is the weld nugget.

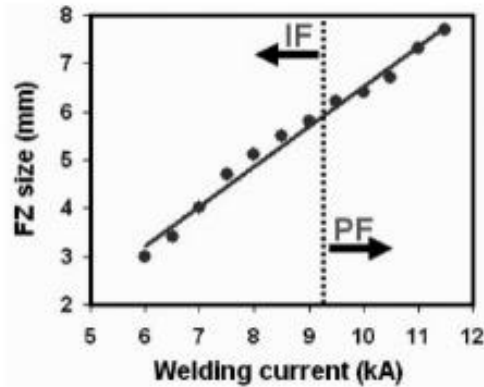


**Figure 8.** Spot weld failure modes at different currents and weld diameters.<sup>[56]</sup>

The spot weld strength and failure modes of Quenching and Partitioning (Q&P) 980 similar steels joints in single pulse RSW and double pulse RSW was studied by Liu et.al[61]. Lap-shear test (and cross tension test which will be discussed later) was used to test the weld samples. This investigation showed that applying a higher secondary current, for instance 7 kA-7.5 kA compared to a constant current of 7 kA, improved the tensile shear strength and failure mode. The weld with constant current of 7 kA, failed with IF due to a small weld developed during welding and crack propagation through the weld and along the sheets interface during lap-shear test. However, with the use of a secondary current within the range of 4.5 kA to 7.5 kA, weld strength increased during the lap shear test and failure mode changed from IF to partial thickness-partial pull-out (PT-PF). Crack propagation during lap-shear test was noticed to penetrate around the circumference of the weld as well as along the partial melting zone (PMZ) and later progressing through the sheet thickness. Zhang et.al[49] used lap-shear test to analyse the spot weld failure on the weld joints made from 1.2 mm DP780 and 1.5 mm DP600 steel sheets. This study reported that during tensile shear test, weld joints first experience shear stress which is parallel to the force direction. The nugget will later rotate in order to realign with the applied force direction. This will lead to a bending moment which in turn creates a tensile stress that is perpendicular to the weld nugget. Even in this study, shear stress was reported to be the driving force for IF and tensile stress being the driving force for PF. However unlike in Pouranvari's work[56], since this study used dissimilar steels, pull-out failure was observed with failure being initiated from the stronger base metal; DP780 in this case. The higher stress concentration on the DP780 side due to the formation of a sharp notch at the sheets interface during lap-shear test initiates crack on the DP780 side which will

later propagate through the base metal to create BM fracture on the D780 side and weld remain intact on the DP600 side.

Duric and Markovic[62] used lap-shear test for 1 and 2 mm thick aluminium and 1 mm thick stainless steel weld joints. This study showed that for dissimilar metals with same thickness, the spot weld failure is dominantly PF while for different thicknesses (aluminium 2mm and steel 1 mm), the spot weld failure is dominantly IF. As in this study, the upper electrode is 5 mm in diameter and the lower electrode is a flat faced back up electrode, which metal is in contact with the upper electrode need additional consideration. The study showed tensile strength is higher for joints with steel in direct contact with the upper electrode compared to joints with aluminium in contact with the upper electrode. Boriwal[63] studied spot weld failure in 0.8 mm thick galvanized steel joints using lap-shear test. This study concluded that welding current and nugget diameters are the main factor for the transition zone of both the IF and PF failure modes similar to the analysis by Pouranvari.[56] The spot weld failure mode transition from IF to PF on 1.7 mm thickness DP600 steel joints for range of welding current, weld time and electrode force as shown in Figure 9 was investigated by Wan et al.[3] This study also used lap-shear test to analyse spot weld failures. A crucial information obtained from this study states that IF of spot weld is usually accompanied by low penetration rate and small size nugget. When the penetration reaches rate of 75% or more, majority failure falls in PF mode. Mousavi et.al[16] used lap shear test to determine the optimum welding parameters to join dissimilar joint of DP600 steel and AISI304 stainless steel. The optimum welding schedule of current 8 kA, 16 cycles weld time and 5 kN electrode force produced PF mode with crack initiation and necking in the thickness direction on the softer base metal i.e. AISI304 stainless steel. To investigate the effect of intermetallic compound (IMC) thickness, nugget diameter and sheet thickness to spot weld failure for joints made from 1.2 mm thick aluminium and 2 mm thick low carbon steel, lap shear test was carried out and the failure modes for different welding schedules were analysed by Chen et al.[64] Three different failure modes were observed in this study. The first failure is a PF with Al button left on the steel surface. The second failure is known as the thickness failure which resembles the IF in similar weld joints, with fracture occurring at the faying surface and the third is a unique failure for Al/steel welds with failure along the IMC layer. The study also concludes when the IMC layer thickness is less than 3  $\mu\text{m}$ , the failure mode is either PF or thickness failure. When the IMC layer thickness is more than 3  $\mu\text{m}$ , the failure will occur with the IMC layer. The study further suggested, to produce a strong and ductile Al/steel weld joint, it is crucial to maintain the thickness of the IMC layer within 3  $\mu\text{m}$  in a lap-shear test.

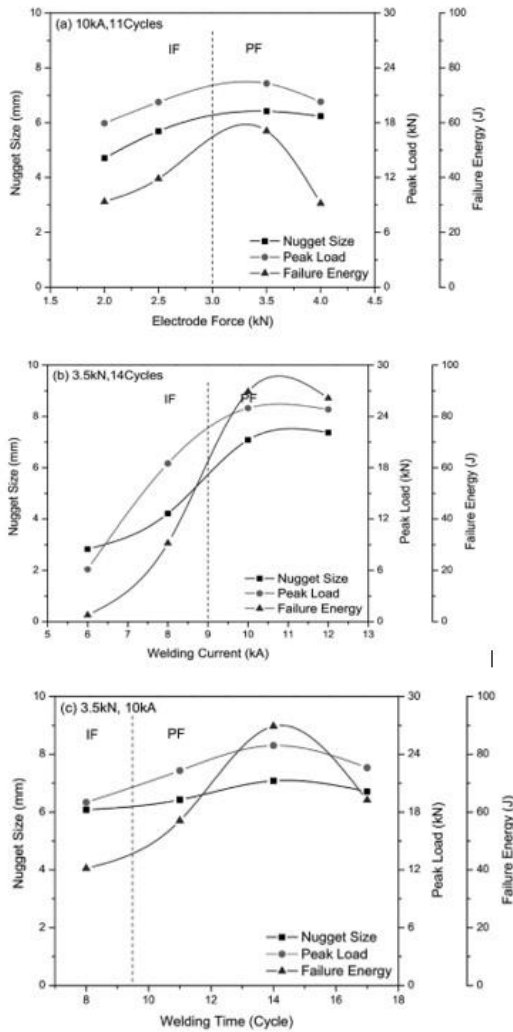


**Figure 9.** Effect of welding parameters to weld failure modes (IF and PF) [3]

To analyse the effect of boron content and welding current to weld joint failure load and mechanism, lap shear test was used by Kong et al.[65] The test samples are made from 1.2 mm thick cold rolled complex steel (CP) sheets containing different amount of boron (B). The lap-shear test showed that for a current range from 5 kA to 10 kA, below 6.4 kA, IF mode was observed regardless of the B content and the variation range of the tensile shear load was narrow. Above 7.4 kA, PF mode was observed, and the tensile shear load increased with increase in current and B content. Also, the study indicated, for weld diameters that failed with IF mode, the change in tensile shear load due to B content is negligible. However, for nugget diameters which failed with PF mode, tensile shear load increased with increase in weld diameter and for the same diameter, load increased with the B content. Kang et.al[66] also contributed in the study of the weldability of dissimilar metals and have used

lap-shear test for strength and weld failure analysis. This work investigated the weldability of aluminium alloy, 1.2 mm AA6022-T4 with 2.0 mm AA6022-T4 and 1.2 mm AA6022-T4 with 2.0 mm interstitial-free (IF) steel. In both joints, welds failed in IF mode during the lap-shear test. The study showed AA6022-T4-IF steel weld joints produced greater weld diameters and higher lap-shear strength as compared to the AA6022-T4- AA6022-T4 weld joints. Tavasolizadeh et.al[67]’s study was different from all the other study discussed above. Unlike other work that used lap-shear test to analyse weld joints made from two metals sheets, this work investigated the use of lap-shear test to analyse weld failure in weld joints made from 3 similar metal sheets. The metal sheet is 1.25 mm thick uncoated load carbon steel and the weld joint is made from 3 sheets stacked together and was identified as the top sheet, middle sheet, and bottom sheet. This study discussed that in a triple sheet stack, weld diameter along the sheet/sheet interface is lower than that of along the geometrical centre of the joint. This type of joint has a high tendency to fail via IF mode during lap-shear test.

The next weld failure test that is quite common especially in the automotive industry is the coach peel test and PF mode is the common failure mode for this test.[68] The continuous bending of the sheet metals in coach-peel test, due to the applied force develops a notch tip closer to the weld, initiating a crack near HAZ. The crack will propagate along sheet thickness causing sheet tearing around weld circumference at a lower load. The stress intensity factor in coach peel to produce a pull-out failure can be divided into stress factor due to bending moment and stress factor due to tensile (axial) force at weld as shown in Equation (4).[69]

$$KI = K_{axial} + K_{moment} = \frac{F}{d\sqrt{\pi d/2}} + \frac{6M}{d^2\sqrt{\pi d/2}} \quad (4)$$

Pouranvari and Marashi[70] concluded the difference in PF mode mechanism for lap-shear and coach-peel tests. In lap-shear test, the PF mode is due to thickness necking while the coach peel test PF mode is due to initiation and propagation of the crack created at the notch tip. This work also presented some crucial information regarding weld strength between both these tests. Firstly, the failure load of spot weld tested with coach peel test was significantly lower than the failure load of the spot weld tested with lap-shear test, for the same weld diameter as shown in Figure 10(a). This attributed to the crack initiation and propagation that was observed in coach peel test. Secondly the displacement of sample prior to failure in the load-displacement graph for coach-peel test is greater than the displacement of sample prior to failure in the load-displacement graph for lap-shear test as in Figure 10(b). This is due to the large sample deformation that was observed in the coach peel test before weld failure occurred. Thirdly, the energy absorption capability of spot welds in coach peel is lower than the same spot welds in lap shear test.

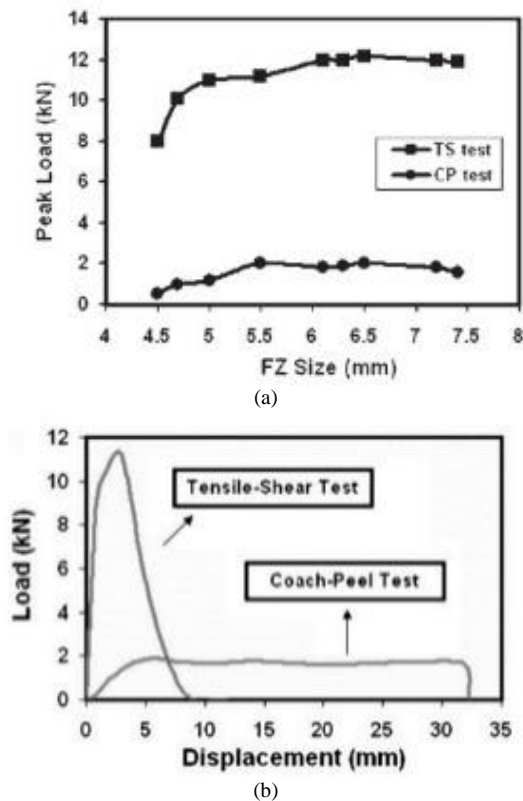


**Figure 10.** (a) Load-displacement curves for lap-shear and coach-peel tests and (b) weld diameters (FZ) and peak loads for lap-shear and coach-peel tests.<sup>[70]</sup>

A comparison study between coach peel test and cross tension test for aluminium and steel joints was discussed in Chen et al.[71] Cross tension test will be discussed in the next section. Similar to Pouranvari and Marashi[70], this work also reported the crack initiation and propagation mechanism prior to spot weld failure during coach peel test. The work further divided the mechanism into 3 stages; a) initial stage; the crack propagates into the Al FZ adjacent to the Al/steel interface and further progressing through the Al sheet top surface resulting in button initiation b) tearing stage; crack propagates circumferentially on both sides of the weld nugget to form button pull out on the steel and finally c) breaking stage; high tensile stress fractured partial Al/steel faying interface and rapidly propagated within the Al sheet until fracture of weld. In a comparison study with the lap-shear test that was carried out by the same authors, Chen et al.[64], lap shear test for Al/steel weld joint showed three fracture modes while for the same Al/steel weld joint, in coach-peel test only one fracture mode was observed i.e partial button pull-out fracture. This work also supported the work of Pouranvari and Marashi [70] indicating that welds, tested with coach peel test had lower peak load compared to the same welds tested with lap shear test. However unlike in Pouranvari and Marashi's work[70], this work reported the welds tested with coach peel test had larger energy absorption capability compared to welds tested with lap-shear test. This difference might possibly be due to the different metals tested by both authors. Yang et.al[72] also investigated the failure modes of spot welds under both cross tension and coach peel test for aluminium alloy (6061-T6 aluminium and 5754-O aluminium) joints

with different thicknesses (1mm, 1.5mm and 2 mm). The peel test samples were made from three sheets of aluminium alloy with two different joint configurations. The IF and PF failure modes were observed for joint configurations with IF failure occurred at the interior of weld nugget and PF mode occurred at the heat affected zone (HAZ) which is referred as the partially melted zone (PMZ) in this work. This work also confirmed that the driving force for IF mode is the tensile stress at the sheets interface and the driving force for PF mode is the shear stress at the weld nugget circumference. Expressions for failure load at IF and PF mode for coach peel test with three sheet thickness were also given as in Equations (5) and (6) respectively

$$F_{IF}^{CP} = P \frac{\pi(\beta d_{IN})^2}{4} \sigma_{FZ} \quad (5)$$

where P – porosity constant (0.9 in this case),  $\beta$  – coefficient =1,  $d_{IN}$  – weld nugget diameter at the interface for a 3-stack joint and  $\sigma_{FZ}$  – tensile strength of the fusion zone.

$$F_{PF}^{CP} \sin\theta = \frac{\pi d_{IN} t \tau_{PFL}}{2} \quad (6)$$

where t = sheet thickness and  $\tau_{PFL}$  – shear strength of the PF location.

Another comparison study between spot weld strength under coach peel test, lap shear test and cross tension test which is yet to be discussed was carried out by Han et.al[73]. Aluminium alloy sheets were used to produce 27 different joint stack-ups (two to four different sheet thicknesses) with differing process parameters. Important information was concluded by this study with regards to the comparison with lap -shear test and coach peel test for the different joint stack-ups with governing metal thickness (GMT); which is the thinnest sheet to be joined in the stack up. The study showed that in the case of the lap-shear test, there is a linear relationship between weld strength and weld diameter with the best fit line having a coefficient of determination (R<sup>2</sup>) of 0.9135. However, in the case of coach-peel test, increase in weld diameter did not lead to significant increase in weld strength with the R<sup>2</sup> for a best fit line being only between -0.13 to 0.1 as the data fall in discrete bands according to the GMT value. Hence this study concluded, unlike in lap shear test, where the shear load is primarily sustained by the weld, in coach-peel, the GMT is a dominant factor governing weld strength. This observation was also supported by the work reported by Yang et al.[72] The effect of weld process variations such as electrode length, current level, sheet metal gap and sheet angle (misalignment) on spot welds made from aluminium steel combination was studied by Chen et al.[74] Coach-peel and lap-shear test were also used to analyse spot weld strength due to these variations. Coach peel samples were found to be insensitive to change in current of about  $\pm 500$  A, however, in lap shear test samples, weld strength increased with increase in current. Both test samples showed sensitivity towards gaps between metal sheets. However, lap shear specimens showed increase in weld strength with introduction of gap between sheets and coach peel specimens showed reduction in weld strength due to introduction of gap between sheets. Misalignment of sheet metals during welding (off normal) was found to affect drastically spot welds in lap-shear test with increase in angle reducing tensile shear strength. However, in coach peel test, the reduction in weld strength due to increase in angle was

not significant. The study also finally concluded at the combination for sheet metal gap and sheet angle was significant for lap-shear test while combination of welding current and sheet angle was significant for coach-peel test.

The final test to analyse spot weld failure is the cross-tension test. Pouranvari[75] and Aghajani and Pouranvari[76] studied the failure modes in similar and dissimilar spot weld joints made from DP600 steel and low carbon steel and joints made from martensitic stainless steels with and without nickel interlayer respectively; using both cross tension test and lap-shear test. The minimum weld diameter required for PF mode during cross tension was observed to be lower than the minimum weld diameter for PF during lap shear test. The reason for this was the difference in stresses the welds will be subjected to during both tests. During cross tension test, the weld circumference will be subjected to shear stress while during lap-shear test, the weld circumference will be subjected to tensile stress. Shear stress and tensile stress in ductile materials can be related either by using von Mises failure criterion or Tresca failure criterion as in Equations (7) and (8):- [77]

$$P_f^{cross\ tension} = 0.735 P_f^{lap\ shear} \quad \text{von Mises} \quad (7)$$

$$P_f^{cross\ tension} = 0.64 P_f^{lap\ shear} \quad \text{Tresca} \quad (8)$$

Hence welds that failed during lap shear tests were found to have a higher strength than weld produced at the same condition but tested under cross tension test. An equation was also suggested as in Equation (9) to calculate the pullout failure load in cross tension test.[78]

$$PPF = \pi dt(\tau)HZ \quad (9)$$

where d- weld diameter, t – sheet thickness and  $(\tau)HAZ$  – shear stress at HAZ.

In Chen et al's work[71], the coach peel test for aluminium and steel weld joints had been discussed in the coach peel section and the cross tension test will be reviewed now. For cross tension test, three different fracture modes were observed while for coach peel test, only one mode was observed as mentioned earlier. The three modes are interfacial fracture mode (IF) where fracture occurred within the IMC layer; partial thickness fracture mode (PTF) where the failure occurred at the Al FZ due to crack initiation and propagation at Al FZ and finally partial button pull-out fracture (PBF or PF in general) where fracture initiated in IMC layer, later propagates towards Al thickness resulting in a small Al button on the steel side. This work also compared the peak load for failure between all three tests discussed, with lap-shear test having the highest peak load or weld strength followed by weld strength from cross tension test and lastly weld strength from coach peel test. This surely supports observation from Pouranvari[75] that stated lap shear test gave a higher weld strength compared to cross tension test.

Yang et.al[72]'s work was earlier discussed in the coach peel section as they have investigated the failure modes of spot welds under both cross tension and coach peel test for aluminium alloy joints with different thicknesses. In the case of cross tension, just as the coach peel test, samples were made from three sheets of aluminium alloy with two joint configurations. As in the case of coach-peel test, in the cross-tension test also, IF and PF were observed in both joint configurations. The IF mode was observed in the interior of the weld nugget mainly due to the formation of

voids in the weld nugget. During cross tension test, crack propagated along the voids and led to IF in spot welds. In Pouranvari's study[75], the IF failure was reported to be controlled by the fracture toughness of the weld or FZ. As fracture toughness in metallurgy refers to the ability of a material containing a crack to resist further fracture, existence of voids in the weld nugget will introduce formation of cracks and reduction the fracture toughness of the weld. In the case of PF of weld, weld fracture was initiated by a tensile stress leading to crack formation along weld circumference. However, the final weld fracture was mainly contributed by the shear stress due to crack propagation along the sheet thickness as reported by Pouranvari[75] and Chen et al.[71]

Expressions for failure load at IF and PF mode for cross tension test with three sheet thickness were also given as in Equations (10) and (11) respectively

$$F_{IF}^{CT} = P \frac{\pi(\alpha d_{IN})^2}{4} \sigma_{FZ} \quad (10)$$

where P – porosity constant (0.9 in this case),  $\alpha$  – coefficient = >1,  $d_{IN}$  – weld nugget diameter at the interface for a 3-stack joint and  $\sigma_{FZ}$  – tensile strength of the fusion zone.

$$F_{PF}^{CT} = \pi d_{IN} t \tau PFL \quad (11)$$

where t = sheet thickness and  $\tau PFL$  – shear strength of the PF location. Equation (10) is the same as Equation (5).

Han et.al[73], whose work on lap shear test and coach peel test for aluminium weld joints of different thicknesses with a GMT was discussed earlier. The same work has also investigated the effect of weld joints made from different joint stack ups to the failure load during cross tension test. The study observed that like the coach peel test, GMT is a dominant factor governing weld strength in cross tension test. However, the load carrying capacity of a spot weld tested in cross tension is twice that for the equivalent spot weld tested with coach peel test. Also, as in the case of the coach peel, the data for relationship between weld diameter to weld strength fall in discrete bands according to the GMT value. But the R2 for a best fit line was between 0.364 to 0.471 which is higher than coach peel test that indicates a certain degree of linear relationship between weld diameter to weld strength in cross tension test. The weldability of 1.1 mm thick Quenching and Partitioning (Q&P) steel with 1.5 mm thick Transformation Induced Plasticity (TRIP) steel was investigated in Spena et al[79]'s work. This work used lap-shear test and cross tension test to analysis spot weld strength and failure in these dissimilar steel joints. Interestingly, this work also reported the same results as Han et.al[73] when analysing the relationship between weld strength and weld diameter for spot welds made from samples of different thickness and tests with lap-shear test and cross tension test. Considering the samples that were tested with the lap shear test, there was a linear relationship between weld diameter and tensile shear strength of weld with coefficient of determination (R2) of 0.82. However, in the case of cross tension test samples, the linear relationship between weld diameter and shear strength fall into three different groups based on the value of the ratio normalised to the spot weld size,  $\alpha$  (kN/mm2). The value of  $\alpha$  is calculated considering the minimum thickness of the steel. The work also showed that spot welds with the same diameter fail with a higher tensile strength compared to the shear strength with failure occurring

mainly at the HAZ of the Q&P steel due to its lower thickness and minimum HAZ hardness compared to TRIP steel.

Subramanian et al.[80] who investigated the effect of constant current and step current/pulse current on weld strength, also used lap-shear test and cross tension test in their analysis. The study reported improvement in spot weld strength in lap shear test and cross tension test by using pulse current compared to the achieved weld strengths for both tests using constant current. Furthermore, the study also showed that for the 5 different welding schedules experimented (one welding schedule with constant current of 12 kA and the remaining four with different current steps with starting current of 12 kA), lap-shear test produced higher spot weld strength compared to the strength measured during cross tension test for a given welding schedule. In addition to that, the failure energy that was calculated from the load -displacement curve also showed that for a given welding schedule; weld failure energy in lap shear test being higher than the weld failure energy in cross tension test.

The weld failure of boron and phosphorous containing steels were investigated using coach-peel test and cross tension test by Amirthalingan et al.[81] The study used three types of steels to form similar spot weld joints; Steel-CP (contains carbon 0.07 wt% and phosphorus 0.08 wt%), Steel-2CP (contains carbon, C 0.14 wt% and phosphorous, P 0.08 wt%) and Steel-CPB (contains carbon, C 0.07 wt%, phosphorous, P 0.08 wt% and boron, B 0.0027 wt%). The thickness of the steels is 1.5 mm. The FZ for all steels had martensite microstructure and Vickers hardness test on the FZ showed that Steel-2CP's FZ have the highest hardness followed by FZs of Steel-CPB and finally Steel-CP. The highest hardness was related to the highest carbon content of Steel-2CP. The coach peel test showed that due to the highest hardness, brittle failure or IF mode was observed in joints made from Steel-2CP. Steel-CP joint showed PPF and joints made from Steel-CPB gave predominantly PF mode. The presence of boron gave better tensile behaviour to the spot weld and Steel-CPB joints had the highest weld strength followed by joints from Steel-CP and Steel-2CP respectively. In the case of cross tension test, Steel-2CP joint again failed by IF while both Steel-CP and Steel-CPB joints failed by PPF. The weld strengths obtained from the cross-tension test also indicated joints of Steel-CPB having the highest strength compared to the Steel-CP and Steel-2CP respectively. A comparison between weld strengths between coach-peel test and cross tension test showed that as with results obtained by Chen et al.[71] and Yang et al.[72], for joints made from either steels, cross tension weld strength was higher than coach peel weld strength.

Cross-tension test was also used by Park et al.[82] to analyse weld failure in medium-Mn TRIP (MT) similar steel joints and MT/DP dissimilar steels joints. The MT similar steel joints were also welded with and without pre-pulse current. The cross-section test showed that for MT similar steels joint with and without pre-pulse current, even though there was a 59% increase in weld diameter with pre-pulse current, the peak loads for failure for both steel joints were very close to each other. This indicated that the increase in weld diameter with the use of pre-pulse current does not give significant effect on the failure load. Also, MT/MT similar joint failed by IF and MT/DP dissimilar joint failed

by PF with failure occurring at MT's HAZ. The difference in fracture path for both joints were observed to be due to the dilution in the FZ.

Based on the above reviews, the driving forces for IF and PF modes in all the three tests discussed are given in Table 1.

**Table 1.** IF and PF driving forces in spot weld for different test samples

Test sample	Driving force	
	IF	PF
Lap-shear	Shear stress at sheet/sheet interface (Mode II)	Tensile stress at weld circumference
Coach peel	Tensile stress at sheet/sheet interface (Mode III)	Bending stress
Cross tension	Opening mode stress intensity (Mode I)	Shear stress at weld circumference.

## 5. Static and dynamic loading

All the tests discussed in the previous section were conducted in the quasi-static loading condition. However since, in real situations, welds commonly fail by means of fatigue fracture, dynamic loading on spot welds required additional consideration. The static and dynamic tensile tests on seven different types of DP and TRIP steels with differences in chemical compositions and thickness were investigated by Ujil et al.[83] The tests were carried out using lap-shear and peel test samples. The static tests were carried out with displacement rate of 10 mm/min. The dynamic tests used an impact-tensile test configuration. Results from this investigation showed that the standard deviation for failure load for static lap-shear test is generally smaller than the failure load standard deviation for dynamic lap-shear test. The same results were also obtained for static and dynamic peel tests. Also, the joints subjected to dynamic loading for both tensile-shear and coach-peel showed higher strength than the joints subjected to static loading. The difference in standard deviation between the failure load of static and dynamic tests was reported to be partly due to the strain rate dependency of the materials. It was also reported in the lap shear tests (static and dynamic), welds predominantly failed in IF mode and peel tests (static and dynamic) predominantly failed in PF mode. The study also showed when the failure load results of static and dynamic loading are combined either for the lap-shear configuration or the peel test configuration, within the grades of steels tested, weld strength of welded joints increased with increase in sheet thickness. Increase in sheet thicknesses was also reported as in Mat Din's study [48], to increase the weld diameters which in turn increases the performance of the welded joints.

Static and dynamic loading of spot weld joints made from DP590 steel was investigated in Song and Huh's study.[59] To create a combined loading condition with an applied failure load that can be decomposed into axial load and shear load, special testing fixtures were used. The fixtures produce different loading angles on the spot welds; 0o, 15o, 30o, 45o, 60o and 75o. Additionally, a pure shear test was also performed by applying the load 90o to the spot weld joints. A quasi static test on all the loading angles were

carried out on a material tensile testing machine with a tensile speed of  $1 \times 10^{-5}$  m/s. Dynamic loading on all the loading angles were carried out on the same machine with three different tensile speeds; 0.01 m/s, 0.1 m/s and 1.2 m/s. Results from this study showed that for a given tensile speed either in quasi static or dynamic condition, maximum failure loads obtained from the load-displacement curves decreased as the loading angles increased till angle of 30°. Further on, the failure loads increased with increase in angle from 45° to 90°. Also, for a particular angle, as the imposed strain rate increased, the maximum failure load from a load-displacement curve increased with increase in tensile speed. Hence dynamic loading will produce higher load compared to quasi static load. The results are the same as the results reported by Ujil et al. [83] when comparing failure loads between quasi static and dynamic loading. In term of the failure mode, loading angle of 0° create pull-out failure with shearing occurring at the circumferential boundary of the nugget. For other angles, the combined axial and shear loading, failure was initiated with the localised necking at the interface between the HAZ and the base metal. The study further showed that when the effect of tensile speeds on the axial load and shear load components were analysed using a logarithmic scale, it was noticed that axial and shear failure loads increase with increase in tensile speed.

The spot weld failure under static loading and cyclic loading (fatigue failure) was investigated by Pizzorni et.al[84]. Two types of lap-shear test samples were prepared; a spot welded (RSW) sample and a hybrid spot weld-epoxy-polyurethane adhesion bonded (RSW-EPUR) sample. DP1000 steel was used as the sheet metals to be joined. The quasi static tensile shear test was conducted with speed of 5 mm/min. Meanwhile the fatigue test was carried out on the same machine using three base load levels (high, medium, low) at a frequency of 10 Hz with sinusoidal variation and constant amplitude. Fatigue test failure criterion: either complete separation of samples or  $1 \times 10^6$  cycles limit, was set for test to stop. Quasi static test results showed that the failure loads for RSW-EPUR samples to be higher than the failure loads for RSW samples. The addition of adhesive to a spot-welded joint was found to increase the resistance to initial shearing of the weld joint hence making the hybrid joint stiffer than the spot welded joint. The overall displacement before failure in the load-displacement curves, however, was the same for both samples and both samples failed by means of PF. In the fatigue tests, RSW-EPUR joints were found to have better resistance to fatigue failure and longer fatigue life compared to RSW joints. Both samples also showed increase in fatigue life with decrease in amplitude of the load cycles. The increase in fatigue life in the hybrid joints compared to welded joints at the same loading condition was due the slow propagation of crack in the adhesive layer. The investigation by Xiao et.al[85] which was similar as the investigation by Pizzorni et.al[84] gave a contradicting result in the case of quasi static experiment. This work used stainless steel and epoxy resin adhesive to form two joint samples; spot welded joint and weld-bonded joint. Unlike in Pizzorni's work[84], the quasi static tensile shear test with the speed of 5 mm/min showed that spot welded joints have higher shear strength than the weld-bonded joints. The adhesive layer in between the stainless-steel sheets were found to raise the contact resistance causing expulsion during welding, hence leading

to reduction in weld strength. The failure mode for the spot-welded joints were base metal tearing/base metal failure while the weld-bonded joints failed by PF. The results in the fatigue test where the no.of cycles before test stops was limited to  $2 \times 10^6$  cycles, however was the same as in Pizzorni's report [84] with the weld-bonded joints have better fatigue performance than the spot welded joints. The other work that supports observation by Pizzorni et.al[84] and Xiao et.al[85] was reported by Fujii et.al.[86] The difference in this work compared to the other two was that the joints were made from three stack of sheets of mild steel and ultra-high strength steel. This work also reported that is the quasi static tensile shear test, the weld-bonded samples for both steels to have higher failure loads compared to the steels spot welded samples. In the fatigue test, just in the case of the previous work, the inclusion of adhesive layer was found to delay the fatigue crack initiation and propagation in the weld-bonded samples hence weld-bonded samples of both steels have longer fatigue life compared to the spot-welded samples.

A comparison study on quasi static lap-shear test, quasi static coach peel test and fatigue test on spot weld joints made from dissimilar metals (1.2 mm thick AA6022-T4 with 2 mm thick IF steel) and similar metals (1.2 mm thick AA6022-T4 with 2 mm thick AA6022-T4) was carried out by Rao et al.[87] The quasi static lap-shear test and coach peel test were performed with speed of 2 mm/min. The fatigue tests were conducted with a constant frequency of 40 Hz for lap-shear and 20 Hz for coach-peel. In both lap-shear test and coach peel test, the dissimilar joint configuration of AA6022-T4-IF produced high fracture load compared to the similar joint configuration of AA6022-T4- AA6022-T4. The reason for this was referred to the weld diameters with dissimilar joints produced bigger welds than similar joints. The results also showed that coach peel tests for both joints produced lower failure loads than the joints tested with lap-shear tests. Referring to the fracture modes, lap-shear tests for the similar and dissimilar joints produced IF and coach-peel tests for both joints produced PF with the weld button on the 1.2 mm AA6022-T4 aluminium sheet. The work also reported that the lap-shear tests were dominated by shear forces and coach-peel tests dominated by bending force. In the case of fatigue test, overall lap-shear joints showed greater fatigue strength compared to coach-peel joints as shown in Figure 11. The fatigue failure was dominated by crack initiation at the notch root opening close to the HAZ which will later propagate through the sheet thickness. The superior fatigue performance in the dissimilar weld joints were deduced to a combination of factors such as weld diameter, HAZ properties and weld nugget hardness.

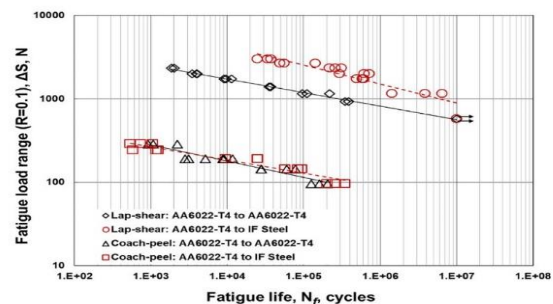


Figure 11. Fatigue life of similar and dissimilar weld joints tested with lap-shear and coach peel [87]

Similar results to Rao et al. [87] was also obtained by Tanegashima et al.[88] where quasi static lap-shear tests produced higher failure strength compared to quasi static coach-peel tests. Lap-shear samples were also reported to have better fatigue strength compared to coach-peel samples. This study also reported fatigue failure occurred due to crack initiation mainly at the notch root opening and further propagated in the thickness direction. The relationship between weld diameters and fatigue life of welds was investigated by Heewon.et.al[89]. The study used two different electrode tip diameters (8 mm and 10 mm) to produce two different weld diameters (5.1 mm and 5.7 mm respectively). Weld joints were made using 1.2 mm thick TRIP steels. The bigger weld diameter was noticed to have a better fatigue strength as in Figure 12. The reason deduced that increase in weld diameter, led to increases joint area. Three different failure modes were observed in this study which depended on the crack initiation and propagation during testing. As reported in Tanegashima et al. work[88], crack initiation was observed at the notch root. However, the way the crack propagated led to three different failure modes. Crack propagation around the nugget gave the PF mode. Crack propagation in the HAZ region, slightly further from the nugget produced the plug failure and finally crack propagation along the sheet thickness produce HAZ failure.

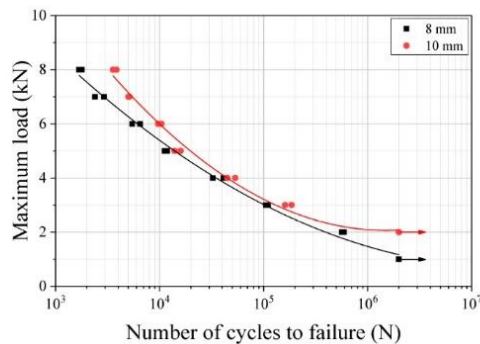


Figure 12. Fatigue life of different weld diameters<sup>[89]</sup>

## 6. Simulation of spot-welding failure

The weld quality and failure analyses reviewed in the previous section are referred to as destructive testing. Destructive testing to measure the spot weld diameter, to determine the weld failure load, process parameter optimization or to analyse the weld failure criterion involved destroying the samples in the testing process. Destructive testing of weld samples usually conducted in a laboratory experimental setup is expensive and time consuming. Also, each test only represents a single loading condition and analyses the effect of combined loading conditions as in the case of the automotive crashes which is not experimentally possible. Advancement in computer technology and knowledge in Finite Element Analysis (FEA) has made many researchers to investigate the use Computer Aided Engineering (CAE) to simulate and analyse spot weld development and failure as a cheaper option to destructive testing and better potential to create complex simulations of weld failure in a crash situation.

Spot welding FEA can be divided into electro-thermal analysis and mechanical-thermal analysis. Figure 13 shows

the RSW FEA procedure. The failure analysis on the spot welds requires an accurate and reliable simulation of the spot welds based on the welding parameters, sheet types and thicknesses as well other process variations such as current shunting, electrode deformation and gap between sheets. Initially, work that have concentrated in the FEA of spot weld development will be reviewed. Two-dimension (2D) axisymmetric models and three dimensional (3D) models have been developed to simulate spot weld formation in DP steels, stainless steels and aluminium steels joints by Vigneshkumar et.al, Baskoro et al, Wan et.al, Jagadeesha, et.al, Lee et.al and Zhao et.al. [90-95] All simulation investigated the spot weld growth in different welding currents and weld time and reported that weld diameter increased with increase in current and weld time with an average error percentage between experimental and simulation of less than 10% indicating good agreement between both results. Figure 14 shows an example of temperature distribution plots for different welding currents, with the distribution of the highest temperature represents the spot weld size (diameter and height).

The simulations of the contact pressure between electrode-sheet interface and sheet-sheet interface during squeeze cycle were investigated by Zhao et.al and Wan et.al.[95, 96] The contact pressure in the workpiece/electrode and workpiece/workpiece interfaces was analysed during the weld cycle and hold cycle. The contact pressure at both interfaces was noticed to increase during weld cycle due to thermal expansion and later decrease due to plastic deformation at the weld centre and eventually changes back to the initial state similar to during squeeze cycle. Concentration of contact pressure at the edge of the contact interfaces was formed after nugget formation which was expected to be beneficial in expulsion prevention. Higher contact pressure at the edge of the electrode was also observed which will lead to electrode plastic deformation.

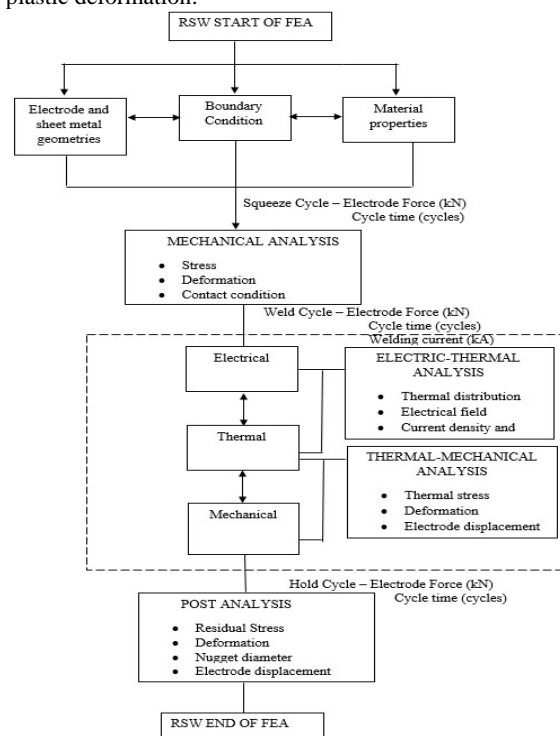
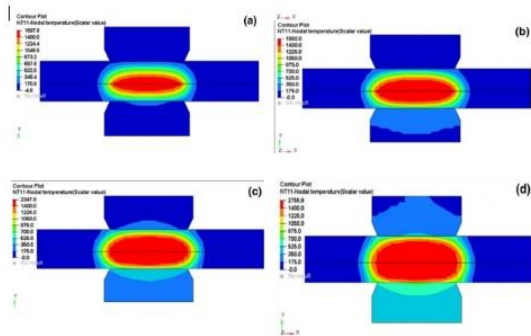


Figure 13. Flowchart of RSW FEA procedure



**Figure 14.** Temperature distribution plots for different welding currents at constant weld time

Numerous works on modelling spot weld joints made of more than two stacks and dissimilar metals have also been carried out. The FEA on nugget growth with three different steels and thickness was analysed by Zhao et al. [97] The study intended to analyse the effect of epoxy adhesive on nugget formation during spot welding. Measurement of the dynamic resistance during spot welding process and weld bonding process showed that existence of adhesive in between sheets increased the contact resistance and initiated nugget formation earlier compared to the spot-welding process which does not have adhesives. The simulations also showed for the same welding parameters, weld-bonding process generated more heat during welding and produced a bigger weld compared to the spot-welding process. The FEA on the spot welding of LITECOR, a hybrid material with a polymer core (0.3 – 1.0 mm thick) between two steel face sheets (each 0.2 – 0.3 mm thick) was developed by Tanco et.al[98]. The modelling of dissimilar joints with aluminium and steel had been studied by Wang et.al, Wan et.al and Du et.al. [99-101] These models concentrated in modelling the IMC thickness at the Al-steel interface and the partial melting zone (PMZ) that is observed in aluminium spot welding which involved unequal thickness. Formation of the PMZ, due to its low thermal conductivity, was observed to function as a heat barrier for molten nugget development. Important information such as the mechanical analysis on sheet deformation and stress/strain rate showed that after welding, the lower electrode which was in contact with the steel showed significant plastic strain compared to the upper electrode that was in contact with aluminium. This indicates the steel side electrode wears out faster than the aluminium side electrode. Further, the analysis on thermal analysis, showed that during welding, steel generated almost 75% of heat while aluminium only generated 4.4% of the total heat used for nugget development and growth in this welding process. All these models agreed well with the experimental results

Sedighi et al.[102] developed a finite element model (FEM) to analyse the effect of sheet thickness on residual stress that exist once the weld nugget has been formed. Aluminium 6061-T6 sheets with four different thicknesses were used in this analysis to form spot weld joints with similar sheet thicknesses. Simulation of residual stress showed that maximum residual stress occurs at the centre of the nugget and diminishes moving towards the edges. Microstructure and thermal gradient were pointed out as the reason for the high residual stress at the weld centre. The analysis also showed that the increase in sheet thickness also

increases the residual stress. This is because when sheet thickness increases, larger nugget diameters are required to create proper weld joint. The larger welds contribute to increase in residual stress due to the increase in tensile residual stress in the nugget during solidification, the more the increase in the compressive residual stress in the adjacent regions. The residual stress on spot weld investigation conducted in Moharrami and Hemmati's work[103] gave a contradictory result compared to Sedighi et al.[102] , yet an accurate representation in term of distribution of residual stress in spot welds after welding. The model analysis showed that the maximum tensile residual stress was located near the edge of the weld nugget. As in Sedighi's report[102], this work also reported that tensile residual stress decreased along the thickness of the sheet. A simulation on the mechanical loading post spot weld also showed plastic deformation along weld nugget due to high stress concentration. The loading analysed with a lap shear test simulation also showed the stress distribution was altered along the direction of loading with tensile stress on one side of the weld and compressive stress on the other side of the weld due to sheet bending.

The effect of electrode tip deformation, current shunting and poor fit on weld nugget development were numerically analysed for using 2D FEMs by Wang et.al, Bi et.al, Yang et.al, Podrzaj et.al.[104-107] The electrode deformations considered in this study were electrode pitting (EP) and electrode tip diameter enlargement (ETDE). Simulation showed that electrodes that had undergone changes in tip morphology either EP or ETDE, produce deterioration in weld strength in comparison to the weld strength achieved by using the normal electrode tip. Both Bi et.al and Yang et.al[105, 106] reported that current shunting is severe when welds are closer to each other hence affecting development of the successive welds. Increasing the weld spacing between the welds reduced the effect of current shunting. The recommended practical weld spacing was 20 mm to 25 mm. Bi also suggested that welds which are closer for instance 16 mm apart may increase the welding current for the second weld, which were found to solve the shunting problem. Even though current shunting to the first weld occurred, the increased current density due to increase in welding current, was found to be able to produce a second weld within the required weld diameters. The concept of increasing welding current was also discussed by Yang who increased the welding current for the third weld when weld spacing between the three welds was 20 mm. Yang also reported that in spot welding, for two spot welds arranged in a line, the current shunting depends only on weld spacing. However, for three spot welds arranged in a triangular pattern, shunting in the third weld depends on the weld spacing and the weld size of prior welds. These models were also validated with experimentation and showed good agreements with experimental results.

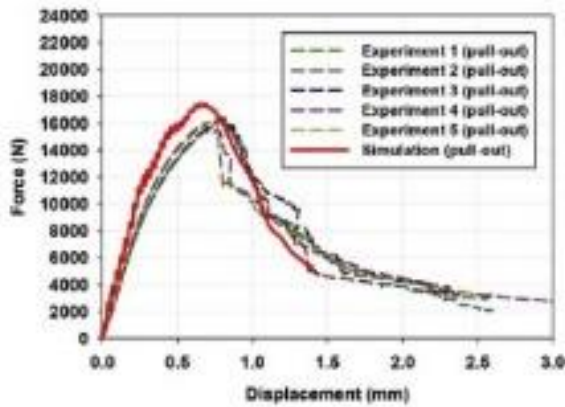
The simulation of spot weld failures involved development of force-displacement curves based on different failure criterion for static loading and dynamic loading and S-N curve for fatigue loading. The FEA on spot weld failure using lap-shear test and U-shape test (cross tension test) was conduct in the work by Chung et.al[108]. The weld failure of similar sheet metal joints in three different types of steels; 1.2 mm thick TRIP980, 1.6 mm thick DP980 and 1.2 mm thick low carbon steel GMW2,

were analysed using both test samples. The analysis considered the hardening deterioration that occurred after ultimate tensile strength (UTS) due to the transformation of micro-voids into macro-cracks especially in ductile sheets. Therefore, stress triaxiality dependent fracture strain and numerical inverse method was used to accurately characterise the failure criterion and hardening behaviour past UTS, which in usual practise would just be extrapolating the hardening behaviour obtained up to the UTS to cover the range beyond UTS. In this study, the simulated force displacement curves corresponded well with the experimental curves for both lap-shear test and U-shape cross tension test. The failure strength and failure modes with both numerical and experimental also agreed well to each other. The averaged errors of the load at the peak between simulation and experiment were 5.92% for lap-shear and 13.5% for U-shape test. However, a larger displacement at fracture error was noticed for both tests with averaged error of 13.2% for lap-shear and 29.8% for U-shape tension test. All experimental tests were conducted under quasi-static loading condition. Noh et al.[109] have also analysed dissimilar steel weld joints DP980-TRIP980 and GMW2-TRIP98 with the same sheet metal thicknesses, failure criterion and test samples as discussed by Chung[108]. This work also showed good agreement between the simulated and experimental load-displacement curves for both lap-shear and U-shaped test samples. The investigation also concluded that the failure in the test coupon was the result of competition between high strength/low ductility zone and low strength/high ductility zone. Figures 15(a) and 15(b) give examples of simulated force-displacement curves for lap-shear test and cross tension test for TRIP980 at 6 kA welding current respectively. Figures 16(a) and 16(b) showed the simulated and experimental failure modes for TRIP980 at 6 kA for lap-shear test and cross tension test, respectively.

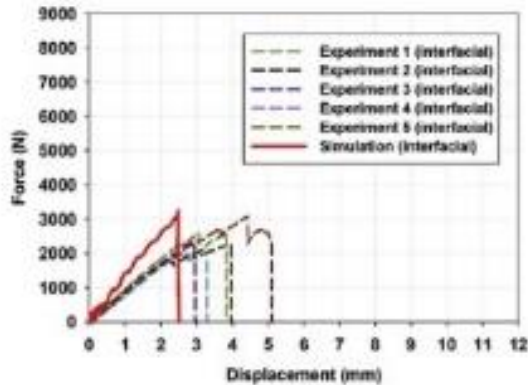
Paveebunvipak and Uthaisangasuk [110] also developed FEMs to simulate the lap-shear and cross-tests for similar and dissimilar steel joints of high strength steel grade 1000 and press hardened (PH) 22MnB5 steel. The study developed the fracture loci for different weld zones, such as base metal (BM), fusion zone (FZ), transition of heat affected zone, and base metal (HAZ/BM) and transition of heat affected zone and fusion zone (HAZ/FZ) by using physical simulation, 2D representative volume element (RVE) and fracture modelling methods. The simulated force-displacement curves and fracture modes which used the developed fracture loci agreed well with the experimental force displacement curves and fracture modes for 1000-1000, PH-PH and 1000-PH steel joints. The effect of the IMC layer's morphology and location to spot weld failure was numerically analysed using FEA by Chen.et.al[111]. This study developed a micro scale model to study the IMC layer's strength in relation to its thickness and location for Al-steel spot welds. A macro model was also developed to analyse the Al-steel spot weld strength using coach peel, lap shear and cross tension test samples. Both models were validated by experimental results. Shear failure model was used to approximate the weld failure. The micro scale model showed that under tensile and shear loading, thin IMC layer ( $<10\mu\text{m}$ ) produced higher failure load compared to thick IMC layer as the crack propagation was obstructed by the large metal remnants in the thin layer.

The stress-displacement curves also showed IMC layer has higher strength in tensile loading compared to shear loading. Also, the highest weld strength in both loading conditions were found to be at the nugget edge rather than the nugget centre as the IMC thickness is relatively thin at the edge. The results of the IMC tensile and shear strengths from the micro-scale model were used to predict the fracture modes in the macro-scale model under coach-peel, lap-shear and cross-tension testing conditions. The load-displacement curves and different fracture modes under lap-shear, coach peel and cross tension agreed to the experimental observation. As reported by other experimental work [75-77,84] with quasi-static loading condition, lap shear test produced the highest spot weld strength, followed the weld strength from cross-tension and finally spot weld from coach-peel test.

The spot weld failure modes using lap-shear, coach peel and cross tension were also studied using FEA by Nguyen et.al.[112] This study used EWK rupture model; a strain damage model for weld failure prediction. Similar to Chen.et.al[111], the spot welds that joined the high strength steels failed either by IF or PF when simulated under the three tests. The load-displacement curves produced by the simulations in this study as well as fracture modes under lap-shear, coach peel and cross tension agreed to the experimental observation. The failure of multiple spot welds during vehicle crash was modelled by Wang et.al[113] using the resultant based failure criterion. The force and moment values for the failure criterion were obtained experimentally via unidirectional loading of single spot weld joints using KSII, coach-peel and torsion tests. The failure criterion was later used in the modelling of a multiple weld joints components subjected to crush test. The peak loads in the load-displacement curves from the crash simulation and experimental crush test results had a relative error of 5%. The simulation however was not able to simulate the local plastic deformation in the sheet that occurred after the peak load hence a difference was observed in the final displacements after the peak loads in both the simulation and experimental load-displacement curves. The use of J-integral fracture criterion to simulate spot weld failure and to calculate the joint's maximum force was investigated by Dorribo et.al.[114] The study concentrated on spot welds in martensite boron steels and considered multiple sheet thickness combinations (0.8 mm, 1.5 mm and 2.0 mm), loading angles (0o-shear loading, 90o-normal loading and 45o- mixed loading) and weld diameters. The failure criterion was able to predict the maximum load for failure in lap shear test and mixed loading test with small relative error percentage compared to experimental maximum load values. However, in the case of the normal test, there was an obvious difference between the simulated and experimental maximum loads and huge error percentage. The results also showed that for a given combination of sheet thicknesses and weld diameter, the peak load for shear test was greater followed by mix-mode and finally normal test as given in Figure 17. The results of mixed mode tests are closer to shear tests, due to the higher relevance of the shear component.

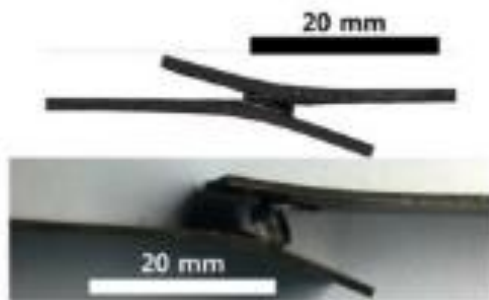


(a)

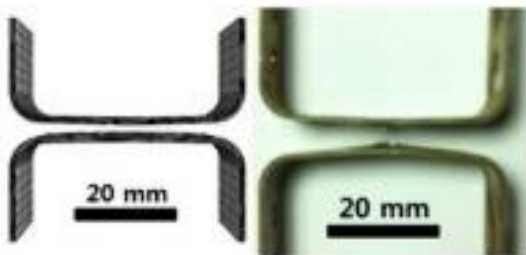


(b)

**Figure 15.** (a) Simulation and experimentation force-displacement curves for lap-shear test and (b) simulation and experimentation force-displacement curves for cross-tension test (TRIP980 6 kA) [108]



(a)



(b)

**Figure 16.** (a) Simulation and experimentation failure modes (PF) for lap-shear test and (b) simulation and experimentation failure modes (IF) for cross-tension test (TRIP980 6 kA) [108]

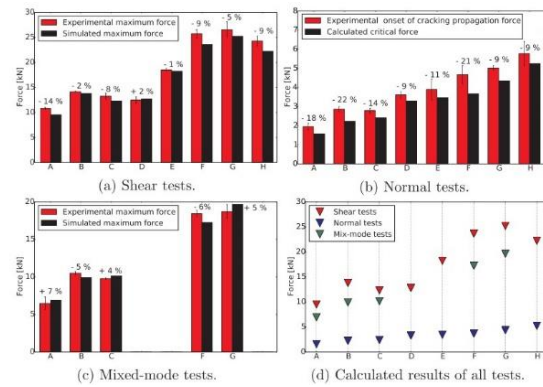


**Figure 17.** Simulation and experimental peak loads for shear test, normal test and mixed mode test [114]

The FEM of hybrid joints of spot weld and epoxy based adhesive was studied by Weiland et.al[115]. KSII cross tension test samples made from 1.4 mm HCT600X DP steel sheets were used in this work. The fracture mode of three different joints; spot weld, adhesive bonded and spot weld-adhesive bonded were modelled by applying tensile (Mode I) and shear (Mode II) loading. A programmed optimization routine based on 10 step calculation schemes was used to simulate the joint fracture and minimize the difference between the mean experimental force-displacement curve and the numerically simulated force-displacement curve. The work reported that the simulated load-displacement curves for all joint types under shear loading agreed well with the experimental data with a percentage error of 9%. However, the simulated load-displacement curves for all joints under tensile loading had a significant error difference of 16% which was attributed to the inability to accurately model the KSII sample deformation at the point of fracture. Another similar work on hybrid joints was also reported by Souza et al.[116] In this work, the numerical models of spot welded joint and spot weld-epoxy adhesive bond joint were tested under lap-shear test. The lap-shear samples were produced using 0.75 mm interstitial free (IF) steel sheets. This work also found good agreement between the simulated load-displacement curves for both joint types with their respective experimental curves. Even though this work did not indicate the fracture model used to simulate the fracture, similar to Weiland et.al's work[115], it also reported higher stiffness and greater failure load in hybrid joints compared to spot welded joints. All the simulations and experimentations reviewed in this section so far were conducted under quasi-static condition.

Researches on FEA of spot weld failure in dynamic loading condition have also been presented. The J-integral fracture criterion, which is associated to crack initiation and propagation was also used by Long et.al[117] to estimate the fatigue life of spot welds of dissimilar metals and unequal thickness joints of DP590 and low carbon steel DC01. Lap-shear test samples were used in this investigation. The study showed that stress intensity factor KI was significantly affected by crack shape and crack length. The developed FEA model in this study was able to estimate closely the fatigue life of lap-shear weld joints to the experimental results at longer life cycle but at lower life cycles, the numerical estimate was twice higher than the experimental results. Chung et al.[108] and Noh et al.[109] also worked on the simulation models to analyse the effect of dynamic loading on spot weld failure.[118] Similar weld

joints of TRIP980 and GMW2 and dissimilar weld joint of TRIP980/GMW2 were analysed using the failure criterion and hardening behaviour discussed in their previous work. Lap-shear and coach-peel test samples were used in this work and dynamic loading speeds of 500 mm/s and 3000 mm/s were applied to these test samples. TRIP980 similar weld joint failed at the FZ via IF for both lap-shear and coach peel tests and the simulation and experimental force-displacement curves and failure modes had a good agreement to each other. The results also showed that the peak load increases with increase in the speed of dynamic loading. GMW2 similar weld joints failed via PF due to the low strength of the BM. However, for GMW2, there was a disagreement in the peak load between simulation and experimentation for both lap-shear and coach peel tests. A variable strain rate-sensitivity model was later used for more accurate prediction of peak load. The dissimilar weld of TRIP980-GMW2 showed only PF for both coupon tests with fracture triggered at the BM of GMW2. As in the case of the GMW2 similar weld joint, variable rate-sensitivity model had to be used to observe better agreement between the simulation and experimental results. The results also showed that the peak load increased with increase in the speed of dynamic loading.

The fatigue life of DP780GI spot weld joints was experimentally and numerically analysed in Wu et.al's work[119]. Lap-shear test and coach peel tests were used in the investigation. Experimental results of weld joint fatigue life in lap-shear and coach peel were similar to results presented in Figure 11. The crack propagation model based on the stress intensity factor (SIF) and Paris Law was used to simulate the crack development in lap-shear and coach-peel tests. In the lap-shear joint, the crack that was initiated at the weld edge and later propagated through the sheet thickness and across the width of the sheet was modelled as a semi oval surface crack. The crack in the coach-peel test, was a combination of interfacial crack and followed by kinked crack. The calculated fatigue life agreed well with the experimental fatigue life for both test samples. Kang et.al[120] developed FEMs to analyse the fatigue life of joints made from spot weld and adhesive and joint made from just adhesive by itself. Lap-shear, coach-peel and cross-tension test samples were used in the finite element modelling. Structural stress equation was used in the development of the S-N curves from the experimental fatigue data for similar steel joints made from DP600 and HSLA340 with lap-shear and coach peel tests. The model was later used to predict the fatigue life of various steel joints made from spot weld and adhesive and joint made from just adhesive only, tested with cross tension test. The simulation showed that there was good agreement between experimental and simulation in the shorter-life region, but difference was observed in the longer-life region. The reasons for this was concluded due to the shortcoming in the model that was developed using lap-shear and coach-peel test samples as well as the inability of the failure criterion to accurately predict the fatigue characteristics of adhesive joints.

## 7. Future work

Review of spot weld failure analyses both, experimentally using test samples as well as numerically

with computational finite element analysis method was carried out. The test samples that are commonly used in experimental analyses were able to analyse spot weld failure in unidirectional loading condition. However, spot weld failure in crash condition is due to combined loading. Patil et.al's [121] FEA model on B-pillar which was subjected to impact loading and Rosch et.al's[122] FEA model on vehicle tow bar subjected to fatigue loading have confirmed that the spot welds are subjected to loads that have components of stresses from the lap-shear, coach-peel and cross tension tests. Figure 18 shows the welds on a B-pillar and the stress components in each weld.

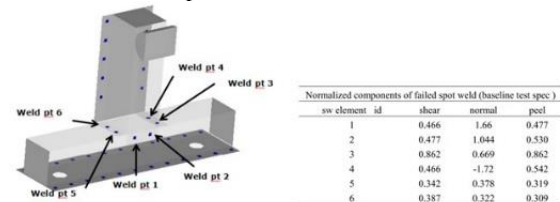
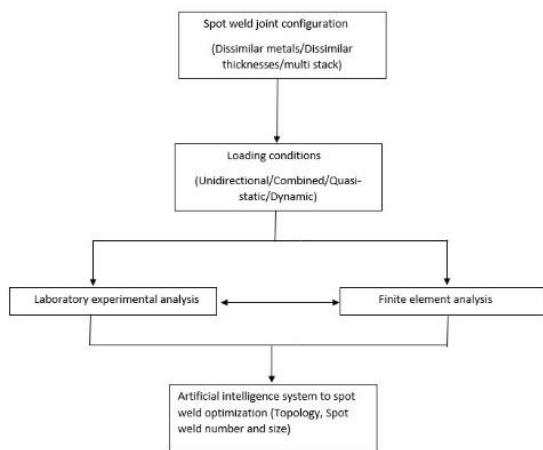


Figure 18. Spot welds and their stress components<sup>[121]</sup>

Hence, the practical spot weld failures may not be accurately analysed in the laboratory experimentation. Furthermore, Li and Feng[123], from their work have concluded that static performance of the BIW in typical working condition is impacted by static torsional stiffness and static bending stiffness. The spot weld failure due to torsional loading have not been extensively analysed in any work. Also experiments on combined loading was attempted by Song.et.al[59] and Dorribo et.al[114], but the joints were only made from similar steels. Therefore, a test sample similar to that used in Wang et al.'s work [113] could be used to conduct analyses on spot weld failure due to torsion. Furthermore, spot weld failure in dissimilar steels with different thickness under combined loading need to be further investigated to address the current automotive design. This may involve requirement for specially designed jigs and fixtures to experimentally impose combined loading on spot welds.

The review also showed that weld bonded joints have better fatigue life compared to spot welded joints. Hence more investigations need to be carried out to explore this joint type. Current work seems to have only concentrated on similar joints. Dissimilar metal weld bonded joints with more than 2 stacks of sheets with different thicknesses need further concentration as this will allow automotive industries to achieve the MML design. In the case of FEA of spot weld failures, in general limited work was found in multi spot weld analysis and spot weld failure due to fatigue loading. Analysing failures involving multiple spot welds subjected to dynamic loading and fatigue loading will be more suitable to be carried out using FEA rather than laboratory experimentation due to the cost and complexity in experimental setup. Ryberg et.al[124] reported that topology optimization and spot weld density optimization are the approaches that have best potential to solve spot weld reduction problem for automotive structures. Both these approaches were evaluated using FEA. Therefore, taking into account these approaches, analyses of multi spot weld failures using combined loading is worth investigating considering the benefits to spot weld reductions. The review have only seen one work on this area; Wang et al.'s work[113] which in fact used quasi static loading.

The FEA of fatigue loading to spot weld failure in dissimilar metal joints and hybrid joints are potential areas for future research. The reviewed work on FEA of hybrid joint used only steel joints subjected to quasi static loading. The ability of hybrid joints to extend fatigue life of spot welds is an important information obtained from this review and further FEA investigation on this type of joint will be beneficial to the automotive industry. Automotive manufacturers are already looking to the potential use of adhesives in automotive manufacturing. However as reported by Kang et al.[120], a separate failure criterion for adhesive is required apart from the failure criterion for the sheets to accurately calculate the fatigue life in FEA. Furthermore, considering the existing limitations in experimental analysis and finite element analyses, development of a hybrid system as in Figure 19, incorporating experimental and numerical analyses to accurately characterise spot weld failure based on the loading conditions and the use of artificial intelligence (AI) systems for spot weld optimization is an area which has a very promising future.



**Figure 19.** Proposed hybrid system for spot weld failure analysis and optimization

## 8. Conclusion

The paper had critically reviewed the analyses of spot weld failures both experimentally and numerically using finite element analysis. The intention of the review is to give comprehensive information on the current practices and research interest related to RSW weld failure analysis. The review has concentrated on the spot weld failures on the current automotive metals, such as Advanced High Strength Steel (AHSS), aluminium and magnesium. Spot weld failure mainly depends on the strength of the spot weld joints which in turn relates to the material weldability, sheet thickness, spot weld positions, welding parameters, material coating and loading types. Currently, due to the need for weight reduction of automotive and increased safety and structural integrity requirement of automotive, dissimilar metal joints; joints made from different metals and thickness are gaining importance in automotive design. Apart from this, automotive industries are also studying the use of adhesive to form hybrid spot weld joints with an

intention to achieve multi-materials lightweight (MML) design.

The required weld joint strength was found to be achieved with the correct combination of welding parameters and balanced heat generation in both metals that are being used to form the weld joint, especially in dissimilar joints. Achieving both conditions will lead to the development of a sound weld nugget to join the metals that being welded. The mechanics of the formation of weld nugget seems different for different metals due to the differences in the materials thermal, mechanical and electrical properties. The joining of AHSS steels involves joining at the sheets interface due to higher dynamic resistance leading to localised metal heating, melting and solidification at the interface creating a weld nugget to join both steels together. The joining of AHSS and aluminium involves formation of intermetallic compound (IMC) layer at the interface and weld nugget only formed on the steel side. Meanwhile for AHSS and magnesium joint, weld nugget is formed on the magnesium side while the metals interface was combined by brazing, soldering and solid state joining.

Weld pull-out failure (PF) is the preferred weld failure in the automotive industries and achieving this failure is attributed to the weld diameter and the types of loading. At present, the ability to achieve PF of weld is being analysed experimentally by using the lap-shear test, coach-peel test and cross-tension test. Each of this test however analyse weld failure on unidirectional loading. Lap shear test produced a greater failure load follow by cross tension test and lastly the coach-peel test. Spot welds are also subjected to quasi-static, dynamic and fatigue loading conditions. The joints subjected to dynamic loading showed higher strength than the joints subjected to static loading. The fatigue life of spot welds can be increased with decrease in amplitude of the load cycles and inclusion of adhesive layer between sheets. Spot weld numerical failure analyses used different failure criteria to simulate the load-displacement curves. Finally, based on the review, future projects were proposed in areas where further research and investigations are required.

## References

- [1] Ambroziak, A.; Korzeniowski, M., Using Resistance Spot Welding for Joining Aluminium Elements in Automotive Industry. *Archives of Civil and Mechanical Engineering* **2010**, *10* (1), 5-13. DOI 10.1016/S1644-9665(12)60126-5
- [2] Yuan, X.; Li, C.; Chen, J.; Li, X.; Liang, X.; Pan, X., Resistance spot welding of dissimilar DP600 and DC54D steels. *Journal of Materials Processing Technology* **2017**, *239*, 31-41. DOI: 10.1016/j.jmatprotec.2016.08.012
- [3] Wan, X.; Wang, Y.; Zhang, P., Effects of Welding Schedules on Resistance Spot Welding of DP600 Steel. *ISIJ International* **2014**, *54* (10), 2375-2379. DOI: 10.2355/isijinternational.54.2375
- [4] Cooke, K. O.; Khan, T. I., Resistance spot welding aluminium to magnesium using nanoparticle reinforced eutectic forming interlayers. *Science and Technology of Welding*

- and Joining **2018**, 23 (4), 271-278. DOI: 10.1080/13621718.2017.1373481
- [5] Pouranvari, M., Critical assessment 27: dissimilar resistance spot welding of aluminium/steel: challenges and opportunities. *Materials Science and Technology* **2017**, 33 (15), 1705-1712. DOI: 10.1080/02670836.2017.1334310
- [6] Winnicki, M.; Małachowska, A.; Korzeniowski, M.; Jasiorski, M.; Baszczuk, A., Aluminium to steel resistance spot welding with cold sprayed interlayer. *Surface Engineering* **2018**, 34 (3), 235-242. DOI: 10.1080/02670844.2016.1271579
- [7] Rajarajan, C.; Sivaraj, P.; Balasubramanian, V., Microstructural analysis of weld nugget properties on resistance spot-welded advance high strength dual phase ( $\alpha + \alpha'$ ) steel joints. *Materials Research Express* **2020**, 7 (1), 016555. DOI: 10.1088/2053-1591/ab654d
- [8] Florea, R. S.; Bammann, D. J.; Yeldell, A.; Solanki, K. N.; Hammi, Y., Welding parameters influence on fatigue life and microstructure in resistance spot welding of 6061-T6 aluminum alloy. *Materials and Design* **2013**, 45, 456-465. DOI: 10.1016/j.matdes.2012.08.053
- [9] Geslain, E.; Rogeon, P.; Pierre, T.; Pouvreau, C.; Cretteur, L., Coating effects on contact conditions in resistance spot weldability. *Journal of Materials Processing Technology* **2018**, 253, 160-167. DOI: 10.1016/j.jmatprotec.2017.11.009
- [10] Safari, M.; Mostaan, H.; Yadegari Kh, H.; Asgari, D., Effects of process parameters on tensile-shear strength and failure mode of resistance spot welds of AISI 201 stainless steel. *The International Journal of Advanced Manufacturing Technology* **2017**, 89 (5), 1853-1863. DOI: 10.1007/s00170-016-9222-z
- [11] Brozek, M.; Novakova, A.; Niedermeier, O., Resistance spot welding of steel sheets of the same and different thickness. *Acta universitatis agriculturae et silviculturae mendelianae brunensis* **2017**, 65 (3), 807-814. DOI: 10.1016/j.jmatprotec.2017.08.035
- [12] Lin, H. C.; Hsu, C. A.; Lee, C. S.; Kuo, T. Y.; Jeng, S. L., Effects of zinc layer thickness on resistance spot welding of galvanized mild steel. *Journal of Materials Processing Technology* **2018**, 251, 205-213. DOI: 10.1016/j.jmatprotec.2017.08.035
- [13] Söderberg, R.; Wärmefjord, K.; Lindkvist, L.; Berlin, R., The influence of spot weld position variation on geometrical quality. *CIRP Annals - Manufacturing Technology* **2012**, 61 (1), 13-16. DOI: 10.1016/j.cirp.2012.03.127
- [14] Ou, Y.; Yueping, L., Quality Evaluation and Automatic Classification in Resistance Spot Welding by Analyzing the Weld Image on Metal Bands by Computer Vision. *International Journal of Signal Processing, Image Processing and Pattern Recognition* **2015**, 8 (5), 301-314. DOI: 10.14257/ijsp.2015.8.5.31
- [15] Vignesh, K.; Elaya Perumal, A.; Velmurugan, P., Optimization of resistance spot welding process parameters and microstructural examination for dissimilar welding of AISI 316L austenitic stainless steel and 2205 duplex stainless steel. *The International Journal of Advanced Manufacturing Technology* **2017**, 93 (1), 455-465. DOI: 10.1007/s00170-017-0089-4
- [16] Mousavi Anijdan, S. H.; Sabzi, M.; Ghoheiti-Hasab, M.; Roshan-Ghiyas, A., Optimization of spot welding process parameters in dissimilar joint of dual phase steel DP600 and AISI 304 stainless steel to achieve the highest level of shear-tensile strength. *Materials Science & Engineering A* **2018**, 726, 120-125. DOI: 10.1016/j.msea.2018.04.072
- [17] Pouranvari, M., Effect of Welding Parameters on the Peak Load and Energy Absorption of Low-Carbon Steel Resistance Spot Welds. *ISRN Mechanical Engineering* **2011**, 1-7. DOI: 10.5402/2011/824149
- [18] Russo Spina, P.; Cortese, L.; De Maddis, M.; Lombardi, F., Effects of Process Parameters on Spot Welding of TRIP and Quenching and Partitioning Steels. *steel research international* **2016**, 87 (12), 1592-1600. DOI: 10.1002/srin.201600007
- [19] Kim, G.-C.; Hwang, I.; Kang, M.; Kim, D.; Park, H.; Kim, Y.-M., Effect of Welding Time on Resistance Spot Weldability of Aluminum 5052 Alloy. *Metals and Materials International* **2019**, 25 (1), 207-218. DOI: 10.1007/s12540-018-0179-3
- [20] Shawon, M.; Gulshan, F.; Kurny, A., Effect of Welding Current on the Structure and Properties of Resistance Spot Welded Dissimilar (Austenitic Stainless Steel and Low Carbon Steel) Metal Joints. *Metallurgical & Materials and Mining Engineering* **2015**, 96 (1), 29-36. DOI: 10.1007/s40033-014-0060-6
- [21] Dwivedi, S. S. S., Optimization of Resistance Spot Welding Process Parameters on Shear Tensile Strength of SAE 1010 steel sheets Joint using Box-Behnken Design. *Jordan Journal of Mechanical and Industrial Engineering* 2016, 10 (2), 115-122.
- [22] Muhammad, N.; Manurung, Y. H. P.; Hafidzi, M.; Abas, S. K.; Tham, G.; Haruman, E., Optimization and modeling of spot welding parameters with simultaneous multiple response consideration using multi-objective Taguchi method and RSM. *Journal of Mechanical Science and Technology* **2012**, 26 (8), 2365-2370. DOI: 10.1007/s12206-012-0618-x
- [23] Wan, X.; Wang, Y.; Zhao, D., Multiple Quality Characteristics Prediction and Parameter Optimization in Small-Scale Resistance Spot Welding. *Arabian Journal for*

- Science and Engineering* **2016**, 41 (5), 2011-2021. DOI: 10.1007/s13369-016-2061-2
- [24] Thakur, A.; Nandedkar, V., Optimization of the Resistance Spot Welding Process of Galvanized Steel Sheet Using the Taguchi Method. *Arabian Journal for Science and Engineering* **2014**, 39 (2), 1171-1176. DOI: 10.1007/s13369-013-0634-x
- [25] Feujofack, K.; Jahazi, M.; Osmani, D., Optimization of resistance spot welding process applied to A36 mild steel and hot dipped galvanized steel based on hardness and nugget geometry. *The International Journal of Advanced Manufacturing Technology* **2020**, 106 (5-6), 2477-2491. DOI: 10.1007/s00170-019-04707-w
- [26] Wan, X.; Wang, Y.; Fang, C., Welding Defects Occurrence and Their Effects on Weld Quality in Resistance Spot Welding of AHSS Steel. *ISIJ International* **2014**, 54 (8), 1883-1889. DOI: 10.2355/isijinternational.54.1883
- [27] Zhao, D.; Wang, Y.; Liang, D.; Zhang, P., An investigation into weld defects of spot-welded dual-phase steel. *The International Journal of Advanced Manufacturing Technology* **2017**, 92 (5), 3043-3050. DOI: 10.1007/s00170-017-0398-7
- [28] Zhou, K.; Yao, P., Overview of recent advances of process analysis and quality control in resistance spot welding. *Mechanical Systems and Signal Processing* **2019**, 124, 170-198. DOI: 10.1016/j.ymssp.2019.01.041
- [29] Zhou, K.; Cal, L., Study on effect of electrode force on resistance spot welding process *Journal of Applied Physics* **2014**, 116 (8). DOI: 10.1063/1.4893968
- [30] Zhang, Y.; Shen, J.; Lai, X., Influence of Electrode Force on Weld Expulsion in Resistance Spot Welding of Dual Phase Steel with Initial Gap Using Simulation and Experimental Method. *ISIJ International* **2012**, 52 (3), 493-498. DOI: 10.2355/isijinternational.52.493
- [31] Zhou, K.; Yao, P.; Cai, L., Constant current vs. constant power control in AC resistance spot welding. *Journal of Materials Processing Tech* **2015**, 223, 299-304. DOI: 10.1016/j.jmatprotec.2015.04.016
- [32] Kang, Z.; Lilong, C., A Nonlinear Current Control Method for Resistance Spot Welding. *IEEE/ASME Transactions on Mechatronics* **2014**, 19 (2), 559-569. DOI: 10.1109/TMECH.2013.2251351
- [33] Bin, N.; Yonglin, C.; Hui, Z., Dynamic electrode force control of resistance spot welding robot. 2009; pp 2421-2426. DOI: 10.1109/ROBIO.2009.5420728
- [34] Ikeda, R.; Okita, Y.; Ono, M.; Yasuda, K.; Terasaki, T., Development of advanced resistance spot welding process using control of electrode force and welding current during welding. *Welding International* **2014**, 28 (1), 13. DOI: 10.1080/09507116.2012.715880
- [35] Chang, H.; Choi, D., Effect of profile force on toughness of resistance spot weld joints for ultra high strength steel. *Welding in the World* **2018**, 62 (3), 481-496. DOI: 10.1080/09507116.2012.715880
- [36] Bondarenko, O. F.; Bondarenko, I. V.; Safronov, P. S.; Sydorets, V. M., Current and force control in micro resistance welding machines Review and development. 2013; pp 298-303. DOI: 10.1109/CPE.2013.6601173
- [37] Matsushita, M.; Ikeda, R.; Oi, K., Development of a new program control setting of welding current and electrode force for single-side resistance spot welding. *The International Journal of Materials Joining* **2015**, 59 (4), 533-543. DOI: 10.1007/s40194-015-0228-1
- [38] Arabi, S. H.; Pouranvari, M.; Movahedi, M., Pathways to improve the austenite-ferrite phase balance during resistance spot welding of duplex stainless steels. *Science and Technology of Welding and Joining* **2019**, 24 (1), 8-15. DOI: 10.1080/13621718.2018.1468949
- [39] Shome, M.; Chatterjee, S., Effect of Material Properties on Contact Resistance and Nugget Size during Spot Welding of Low Carbon Coated Steels. *ISIJ International* **2009**, 49 (9), 1384-1391. DOI: DOI: 10.2355/isijinternational.49.1384
- [40] Aktas, S.; Ozsarac, U.; Aslanlar, S., Effect of Spot Welding Parameters on Tensile Properties of DP 600 Steel Sheet Joints. *Materials and Manufacturing Processes* **2012**, 27 (7), 756-764. DOI: 10.1080/10426914.2011.647940
- [41] Aydin, H., The mechanical properties of dissimilar resistance spot-welded DP600–DP1000 steel joints for automotive applications. *Proc IMechE PartD: Journal of Automobile Engineering* **2014**, 1-12. DOI: 10.1177/0954407014547749
- [42] Kishore, K.; Kumar, P.; Mukhopadhyay, G., Resistance spot weldability of galvanized and bare DP600 steel. *Journal of Materials Processing Technology* **2019**, 271, 237-248. DOI: 10.1016/j.jmatprotec.2019.04.005
- [43] Wei, S. T.; Lv, D.; Liu, R. D.; Lin, L.; Xu, R. J.; Guo, J. Y.; Wang, K. Q., Similar and dissimilar resistance spot welding of advanced high strength steels: welding and heat treatment procedures, structure and mechanical properties. *Science and Technology of Welding and Joining* **2014**, 19 (5), 427-435. DOI: 10.1179/1362171814Y.0000000211
- [44] Liu, L.; Xiao, L.; Chen, D. L.; Feng, J. C.; Kim, S.; Zhou, Y., Microstructure and fatigue properties of Mg-to-steel dissimilar resistance spot welds. *Materials and Design* **2013**, 45, 336-342. DOI: 10.1016/j.matdes.2012.08.018
- [45] Manladan, S. M.; Zhang, Y.; Ramesh, S.; Cai, Y.; Luo, Z.; Ao, S.; Arslan, A., Resistance element weld-bonding and resistance spot weld-bonding of Mg alloy/austenitic stainless steel. *Journal of Manufacturing Processes* 2019, 48, 12-30. DOI: 10.1016/j.jmapro.2019.10.005
- [46] Miyamoto, K.; Nakagawa, S.; Sugi, C.; Ogura, T.; Hirose, A., Seal spot welding of steel and aluminium alloy by resistance spot welding: dissimilar metal joining of steel and aluminium alloy by Zn insertion. *Welding International* 2016, 30 (9), 675-687. DOI: 10.1080/09507116.2016.1142189
- [47] Sakiyama, T.; Naito, Y.; Miyazaki, Y.; Nose, T., Dissimilar Metal Joining Technologies for Steel Sheet and Aluminum Alloy Sheet in Auto Body. NIPPON STEEL TECHNICAL REPORT 2013, 103, 91-98.
- [48] Mat Din, N. A.; Zuhailawati, H.; Anasyida, A., Resistance Spot Welding of AA5052 Sheet Metal of Dissimilar Thickness. Anasyida, A., Ed. 2016; Vol. 114, pp 12126-12133. DOI: 10.1088/1757-899X/114/1/012126

- [49] Zhang, H.; Qiu, X.; Xing, F.; Bai, J.; Chen, J., Failure analysis of dissimilar thickness resistance spot welded joints in dual-phase steels during tensile shear test. *Materials and Design* 2014, 55, 366-372. DOI: 10.1016/j.matdes.2013.09.040
- [50] Pouranvari, M.; Mousavizadeh, S. M.; Marashi, S. P. H.; Goodarzi, M.; Ghorbani, M., Influence of fusion zone size and failure mode on mechanical performance of dissimilar resistance spot welds of AISI 1008 low carbon steel and DP600 advanced high strength steel. *Materials & Design* 2011, 32 (3), 1390-1398. DOI: 10.1016/j.matdes.2010.09.010
- [51] Jawaid, R., Failure Study of Two Dissimilar Steels Joined by Spot Welding Technique. *Key Engineering Materials* 2018, 778, 262-267. DOI: 10.4028/www.scientific.net/KEM.778.262
- [52] Huin, T.; Dancette, S.; Fabregue, D.; Dupuy, T., Investigation of the Failure of Advanced High Strength Steels Heterogeneous Spot Welds. *Metals* 2016, 6 (5), 1-19. DOI: 10.3390/met6050111
- [53] Pouranvari, M.; Marashi, S. P. H.; Safanama, D. S., Failure mode transition in AHSS resistance spot welds. Part II: Experimental investigation and model validation. *Materials Science & Engineering A* 2011, 528 (29-30), 8344-8352. DOI: 10.1016/j.msea.2011.08.016
- [54] Xu, F.; Sun, G.; Li, G.; Li, Q., Failure analysis for resistance spot welding in lap-shear specimens. *International Journal of Mechanical Sciences* 2014, 78, 154-166. DOI: 10.1016/j.ijmecs.2013.11.011
- [55] Chen, F.; Sun, S.; Ma, Z.; Tong, G.; Huang, X., Effect of weld nugget size on failure mode and mechanical properties of microscale resistance spot welds on Ti-1Al-1Mn ultrathin foils. *Advances in Mechanical Engineering* 2018, 10 (7), 1-10. DOI: 10.1177/1687814018785283
- [56] Pouranvari, M., On the Failure Mode of Resistance Spot Welded Hsla 420 Steel Archives of Metallurgy and Materials 2013, 58 (1), 67-72. DOI: 10.2478/v10172-012-0152-y
- [57] Abadi, M.; Pouranvari, M., Failure-mode transition in resistance spot welded DP780 advanced high-strength steel: Effect of loading conditions. *Materials and Technology*. 2014, 48 (1), 67-71.
- [58] Zhao, D.; Wang, Y.; Liang, D.; Zhang, P., Modeling and process analysis of resistance spot welded DP600 joints based on regression analysis. *Materials & Design* 2016, 110, 676-684. DOI:10.1016/j.matdes.2016.08.038
- [59] Song, J. H.; Huh, H., Influence of Tensile Speeds on the Failure Loads of the DP590 Spot Weld under Various Combined Loading Conditions. *Advances in Materials Science and Engineering* 2015, 2015. DOI: 10.1155/2015/297915
- [60] Pouranvari, M.; Marashi, S., Factors affecting mechanical properties of resistance spot welds. *Materials Science and Technology* 2010, 26 (9), 1137. DOI: 10.1179/174328409X459301
- [61] Liu, X. D.; Xu, Y. B.; Misra, R. D. K.; Peng, F.; Wang, Y.; Du, Y. B., Mechanical properties in double pulse resistance spot welding of Q&P 980 steel. *Journal of Materials Processing Technology* 2019, 263, 186-197. DOI: 10.1016/j.jmatprotec.2018.08.018
- [62] Aleksija, Đ.; Biljana, M., Failure mode and strength analyses of resistance spot weld joints of aluminium and austenitic stainless steel sheet. *Applied Engineering Letters* 2018, 3 (1), 6-12. DOI: 10.18485/aeletters.2018.3.1.2
- [63] Boriwal, L.; Sarviya, R. M.; Mahapatra, M. M., Failure modes of spot welds in quasi – static tensile – shear loading of coated steel sheets. *Materials Today: Proceedings* 2017, 4 (2), 3672-3677. DOI: 10.1016/j.matpr.2017.02.261
- [64] Chen, N.; Wang, H.-P.; Carlson, B. E.; Sigler, D. R.; Wang, M., Fracture mechanisms of Al/steel resistance spot welds in lap shear test. *Journal of Materials Processing Technology* 2017, 243, 347-354. DOI: 10.1016/j.jmatprotec.2016.12.015
- [65] Kong, J. P.; Han, T. K.; Chin, K. G.; Park, B. G.; Kang, C. Y., Effect of boron content and welding current on the mechanical properties of electrical resistance spot welds in complex-phase steels. *Materials and Design* 2014, 54, 598-609. DOI: 10.1016/j.matdes.2013.08.098
- [66] Kang, J.; Rao, H. M.; Sigler, D. R.; Carlson, B. E., Tensile and Fatigue Behaviour of AA6022-T4 to IF Steel Resistance Spot Welds. *Procedia Structural Integrity* 2017, 5, 1425-1432. DOI: 10.1016/j.prostr.2017.07.207
- [67] Tavasolizadeh, A.; Marashi, S. P. H.; Pouranvari, M., Mechanical performance of three thickness resistance spot welded low carbon steel. *Materials Science and Technology* 2011, 27 (1), 219-224. DOI: 10.1179/174328409X441265
- [68] Summerville, C.; Compston, P.; Doolan, M., A comparison of resistance spot weld quality assessment techniques. *Procedia Manufacturing* 2019, 29, 305-312. DOI: 10.1016/j.promfg.2019.02.142
- [69] Kyung Min Lee; Dong Woon Han; Kim, H. K., Fatigue strength evaluation of self-piercing riveted cold rolled steel joints under mixed mode loading conditions. *International Journal of Engineering and Technology* 2016, 8 (4), 1826-1831. DOI: 10.21817/ijet/2016/v8i4/160804166
- [70] Pouranvari M; P, M., Failure of resistance spot welds: Tensile shear versus coach peel loading conditions. *Ironmaking & Steelmaking* 2012, 39 (2), 104-111. DOI: 10.1179/1743281211Y.0000000066
- [71] Chen, N.; Wang, H.-P.; Carlson, B. E.; Sigler, D. R.; Wang, M., Fracture mechanisms of Al/steel resistance spot welds in coach peel and cross tension testing. *Journal of Materials Processing Tech.* 2018, 252, 348-361. DOI: 10.1016/j.jmatprotec.2017.09.035
- [72] Yang Li; He Shan; Yu Zhang; Luo, Z., Failure mode of spot welds under cross-tension and coach-peel loads. *Welding Journal* 2017, 96 (11), 413-420.
- [73] Han, L.; Thornton, M.; Boomer, D.; Shergold, M., A correlation study of mechanical strength of resistance spot welding of AA5754 aluminium alloy. *Journal of Materials Processing Technology* 2011, 211 (3), 513-521. DOI: 10.1016/j.jmatprotec.2010.11.004
- [74] Chen, C.; Kong, L.; Wang, M.; Haselhuhn, A. S.; Sigler, D. R.; Wang, H.-P.; Carlson, B. E., The robustness of Al-steel resistance spot welding process. *Journal of Manufacturing Processes* 2019, 43, 300-310. DOI: 10.1016/j.jmapro.2019.02.030

- [75] Pouranvari, M., Susceptibility to interfacial failure mode in similar and dissimilar resistance spot welds of DP600 dual phase steel and low carbon steel during cross-tension and tensile-shear loading conditions. *Materials Science & Engineering A* **2012**, *546*, 129-138. DOI: 10.1016/j.msea.2012.03.040
- [76] Aghajani, H.; Pouranvari, M., A pathway to produce strong and tough martensitic stainless steels resistance spot welds. *Science and Technology of Welding and Joining* **2019**, *24* (3), 185-192. DOI: 10.1007/s11661-019-05443-2
- [77] Chao, Y., Ultimate strength and failure mechanism of resistance spot weld subjected to tensile, shear, or combined tensile/shear loads. *Journal of Engineering Materials and Technology (Transactions of the ASME)* **2003**, *125* (2), 125-132. DOI: 10.1115/1.1555648
- [78] Pouranvari, M.; Marashi, S. P. H., Failure Mode Transition in AISI 304 Resistance Spot Welds. *Welding Journal* **2012**, *91* (11), 303-309.
- [79] Spina, P.; Maddis, M.; D'Antonio, G.; Lombardi, F., Weldability and Monitoring of Resistance Spot Welding of Q&P and TRIP Steels. *Metals* **2016**, *6* (11), 270. DOI: 10.3390/met6110270
- [80] Subramanian, A.; Senthil, P. V.; Jabaraj, D. B.; Devakumar, D., Improving mechanical performance of resistance spot welded joints of AISI 409M steel by double pulse current. *Materials Today: Proceedings* **2019**, *16*, 949-955. DOI: 10.1016/j.matpr.2019.05.181
- [81] Amirthalingam, M.; van Der Aa, E.; Kwakernaak, C.; Hermans, M.; Richardson, I., Elemental segregation during resistance spot welding of boron containing advanced high strength steels. *Weld. World* **2015**, *59* (5), 743-755. DOI: 10.1007/s40194-015-0250-3
- [82] Park, G.; Kim, K.; Uhm, S.; Lee, C., A comparison of cross-tension properties and fracture behavior between similar and dissimilar resistance spot-weldments in medium-Mn TRIP steel. *Materials Science and Engineering: A* **2019**, *752*, 206-216. DOI: 10.1016/j.msea.2019.03.023
- [83] Uijl, N.; Moolevliet, T.; Mennes, A.; Ellen, A.; Smith, S.; Veldt, T.; Okada, T.; Nishibata, H.; Uchihara, M.; Fukui, K., Performance of Resistance Spot-Welded Joints in Advanced High-Strength Steel in Static and Dynamic Tensile Tests. *Welding in the World* **2012**, *56* (7), 51-63. DOI: 10.1007/BF03321365
- [84] Pizzomi, M.; Lertora, E.; Mandolino, C.; Gambaro, C., Experimental investigation of the static and fatigue behavior of hybrid ductile adhesive-RSWelded joints in a DP 1000 steel. *International Journal of Adhesion and Adhesives* **2019**, *95*, 102400. DOI: 10.1016/j.ijadhadh.2019.102400
- [85] Xiao, Z.; Zeng, K.; He, X.; Zhang, L., Fatigue strength and failure analysis of weld-bonded joint of stainless steel. *The Journal of Adhesion* **2019**, *95* (3), 1-17. DOI: 10.1080/00218464.2017.1414605
- [86] Fujii, T.; Tohgo, K.; Suzuki, Y.; Yamamoto, T.; Shimamura, Y., Fatigue strength and fatigue fracture mechanism of three-sheet spot weld-bonded joints under tensile-shear loading. *International Journal of Fatigue* **2016**, *87*, 424-434. DOI: 10.1016/j.ijfatigue.2016.02.023
- [87] Rao, H. M.; Kang, J.; Shi, L.; Sigler, D. R.; Carlson, B. E., Effect of specimen configuration on fatigue properties of dissimilar aluminum to steel resistance spot welds. *International Journal of Fatigue* **2018**, *116*, 13-21. DOI: 10.1016/j.ijfatigue.2018.06.009
- [88] Tanegashima, R.; Akebono, H.; Sugeta, A., Fatigue life estimation based on fracture mechanics of single spot welded joints under different loading modes. *Engineering Fracture Mechanics* **2017**, *175*, 115-126. DOI: 10.1016/j.engfracmech.2017.01.031
- [89] Heewon, C.; Sangwoo, N.; Insung, H.; Je Hoon, O.; Munjin, K.; Young-Min, K., Fatigue Behaviors of Resistance Spot Welds for 980 MPa Grade TRIP Steel. *Metals* **2019**, *9* (10), 1086. DOI: 10.3390/met9101086
- [90] Vigneshkumar, M.; Varthanan, P. A.; Ambrose Raj, Y. M., Finite Element-Based Parametric Studies of Nugget Diameter and Temperature Distribution in the Resistance Spot Welding of AISI 304 and AISI 316L Sheets. *Transactions of the Indian Institute of Metals* **2019**, *72* (2), 429-438. DOI: 10.1007/s12666-018-1494-6
- [91] Baskoro, A. S.; Edyanto, A.; Amat, M. A.; Muzaki, H., Study on Nugget Growth in Resistance Spot Welding of Thin Aluminum A1100 Using Welding Simulation. *Materials Science Forum* **2018**, *929*, 191-199. DOI: 10.4028/www.scientific.net/MSF.929.191
- [92] Wan, X.; Wang, Y.; Zhang, P., Modelling the effect of welding current on resistance spot welding of DP600 steel. *Journal of Materials Processing Technology* **2014**, *214* (11), 2723-2729. DOI: 10.1016/j.jmatprotec.2014.06.009
- [93] Jagadeesha T, T.; Jothi, T., Studies on the influence of process parameters on the AISI 316L resistance spot-welded specimens. *The International Journal of Advanced Manufacturing Technology* **2017**, *93* (1), 73-88. DOI: 10.1007/s00170-015-7693-y
- [94] Lee, Y.; Jeong, H.; Park, K.; Kim, Y.; Cho, J., Development of numerical analysis model for resistance spot welding of automotive steel. *Journal of Mechanical Science and Technology* **2017**, *31* (7), 3455-3464. DOI: 10.1007/s12206-017-0634-y
- [95] Zhao, D.; Wang, Y.; Zhang, P.; Liang, D., Modeling and Experimental Research on Resistance Spot Welded Joints for Dual-Phase Steel. *Materials* **2019**, *12* (7), 1-16. DOI: 10.3390/ma12071108
- [96] Wan, X.; Wang, Y.; Zhang, P., Numerical simulation on deformation and stress variation in resistance spot welding of dual-phase steel. *The International Journal of Advanced Manufacturing Technology* **2017**, *92* (5), 2619-2629. DOI: 10.1007/s00170-017-0191-7
- [97] Zhao, Y.; Zhang, Y.; Lai, X., Effect of Epoxy Adhesive on Nugget Formation in Resistance Welding of SAE1004/DP600/DP780 Steel Sheets. *Materials* **2018**, *11* (10). DOI: 10.3390/ma11101828
- [98] Tanco, J. S.; Nielsen, C. V.; Chergui, A.; Zhang, W.; Bay, N., Weld nugget formation in resistance spot welding of new lightweight sandwich material. *The International Journal of Advanced Manufacturing Technology* **2015**, *80* (5-8), 1137-1147. DOI: 10.1007/s00170-015-7108-0.

- [99] Wang, J.; Wang, H. P.; Lu, F.; Carlson, B. E.; Sigler, D. R., Analysis of Al-steel resistance spot welding process by developing a fully coupled multi-physics simulation model. *International Journal of Heat and Mass Transfer* **2015**, *89*, 1061-1072. DOI: 10.1016/j.ijheatmasstransfer.2015.05.086
- [100] Wan, Z.; Wang, H.-P.; Wang, M.; Carlson, B. E.; Sigler, D. R., Numerical simulation of resistance spot welding of Al to zinc-coated steel with improved representation of contact interactions. *International Journal of Heat and Mass Transfer* **2016**, *101*, 749-763. DOI: 10.1016/j.ijheatmasstransfer.2016.05.023
- [101] Du, H.; Bi, J.; Zhang, Y.; Wu, Y.; Li, Y.; Luo, Z., The role of the partial melting zone in the nugget growth process of unequal-thickness dissimilar aluminum alloy 2219/5A06 resistance spot welding. *Journal of Manufacturing Processes* **2019**, *45*, 304-311. DOI: 10.1016/j.jmapro.2019.06.026
- [102] Sedighi, M.; Afshari, D.; Nazari, F., Investigation of the effect of sheet thickness on residual stresses in resistance spot welding of aluminum sheets. *Proc IMechE Part C: J Mechanical Engineering Science* **2018**, *232* (4), 621-628. DOI: 10.1177/0954406216685124
- [103] Moharrami, R.; Hemmati, B., Numerical stress analysis in resistance spot-welded nugget due to post-weld shear loading. *Journal of Manufacturing Processes* **2017**, *27*, 284-290. DOI: 10.1016/j.jmapro.2017.05.007
- [104] Wang, B.; Hua, L.; Wang, X.; Song, Y.; Liu, Y., Effects of electrode tip morphology on resistance spot welding quality of DP590 dual-phase steel. *The International Journal of Advanced Manufacturing Technology* **2016**, *83* (9), 1917-1926. DOI: 10.1007/s00170-015-7703-0
- [105] Bi, J.; Song, J.; Wei, Q.; Zhang, Y.; Li, Y.; Luo, Z., Characteristics of shunting in resistance spot welding for dissimilar unequal-thickness aluminum alloys under large thickness ratio. *Materials & Design* **2016**, *101*, 226-235. DOI: 10.1016/j.matdes.2016.04.023
- [106] Yang, L.; Bi, J.; Zhang, Y.; Luo, Z.; Liu, W., Shunting characteristics in triangular arranged resistance spot welding of dissimilar unequal-thickness aluminum alloys. *The International Journal of Advanced Manufacturing Technology* **2017**, *91* (5-8), 2447-2454. DOI: 10.1007/s00170-016-9926-0
- [107] Podrżaj, P.; Jerman, B.; Simončič, S., Poor fit-up condition in resistance spot welding. *Journal of Materials Processing Technology* **2016**, *230*, 21-25. DOI: 10.1016/j.jmatprotec.2015.11.009
- [108] Chung, K.; Noh, W.; Yang, X.; Han, H. N.; Lee, M.-G., Practical failure analysis of resistance spot welded advanced high-strength steel sheets. *International Journal of Plasticity* **2017**, *94*, 122-147. DOI: 10.1016/j.ijplas.2016.10.010
- [109] Noh, W.; Kim, W.; Yang, X.; Kang, M.; Lee, M.-G.; Chung, K., Simple and effective failure analysis of dissimilar resistance spot welded advanced high strength steel sheets. *International Journal of Mechanical Sciences* **2017**, *121*, 76-89. DOI: 10.1016/j.ijmecsci.2016.12.006
- [110] Paveebunvipak, K.; Uthaisangsuk, V., Microstructure based modeling of deformation and failure of spot-welded advanced high strength steels sheets. *Materials & Design* **2018**, *160*, 731-751. DOI: 10.1016/j.matdes.2018.09.052
- [111] Chen, J.; Feng, Z.; Wang, H.-P.; Carlson, B. E.; Brown, T.; Sigler, D., Multi-scale mechanical modeling of Al-steel resistance spot welds. *Materials Science and Engineering: A* **2018**, *735*, 145-153. DOI: 10.1016/j.msea.2018.08.039
- [112] Nguyen, N.; Kim, D.; Song, J.; Kim, K.; Lee, I.; Kim, H., Numerical prediction of various failure modes in spotwelded metals. *International Journal of Automotive Technology* **2012**, *13* (3), 459-467. DOI: 10.1007/s12239-012-0043-2
- [113] Wang, W.; Zhu, Q.; Liu, C.; Wei, X., An investigation on the resultant-based failure criterion for resistance spot welding joint in crush test. *International Journal of Crashworthiness* **2019**, *24* (2), 152-162. DOI: 10.1080/13588265.2017.1421012
- [114] Dorribo, D.; Greve, L.; Díez, P.; Arias, I.; Larráyoz-Izcara, X., Numerical estimation of the bearing capacity of resistance spot welds in martensitic boron steels using a J-integral fracture criterion. *Theoretical and Applied Fracture Mechanics* **2018**, *96*, 497-508. DOI: 10.1016/j.tafmec.2018.06.006
- [115] Weiland, J.; Debruyne, S.; Vandepitte, D.; Pulm, M.; Schiebahn, A.; Reisgen, U., Stiffness and strength analysis of hybrid adhesive bonded - resistance spot welded sandwich samples by means of virtual FE testing. *The Journal of Adhesion* **2019**, *95* (5-7), 543-557. DOI: 10.1080/00218464.2018.1553713
- [116] Souza, J. P. B.; Aguiar, R. A. A.; Costa, H. R. M.; Reis, J. M. L.; Pacheco, P. M. C. L., Numerical modelling of the mechanical behavior of hybrid joint obtained by spot welding and bonding. *Composite Structures* **2018**, *202*, 216-221. DOI: 10.1016/j.compstruct.2018.01.066
- [117] Long, H.; Hu, Y.; Jin, X., Stress intensity factor solutions and fatigue estimation for dual phase and low-carbon steel spot weld. *Theoretical and Applied Fracture Mechanics* **2018**, *96*, 408. DOI: 10.1016/j.tafmec.2018.06.003
- [118] Noh, W.; Koh, Y.; Chung, K.; Song, J.-H.; Lee, M.-G., Influence of dynamic loading on failure behavior of spot welded automotive steel sheets. *International Journal of Mechanical Sciences* **2018**, *144*, 407-426. DOI: 10.1016/j.ijmecsci.2018.06.009
- [119] Wu, G.; Li, D.; Su, X.; Peng, Y.; Shi, Y.; Huang, L.; Huang, S.; Tang, W., Experiment and modeling on fatigue of the DP780GI spot welded joint. *International Journal of Fatigue* **2017**, *103*, 73-85. DOI: 10.1016/j.ijfatigue.2017.05.017
- [120] Kang, H.; Li, Z.; Khosrovaneh, A. K.; Kang, B.; Li, Z., Fatigue Life Predictions of Adhesive Joint of Sheet Steels. *Procedia Engineering* **2015**, *133* (C), 518-527. DOI: 10.1016/j.proeng.2015.12.623
- [121] Patil, S. A.; Baratzadeh, F.; Lankarani, H., Modeling of the Weld Strength in Spot Weld Using Regression Analysis of the Stress Parameters based on the Simulation Study. *Journal of Materials Science Research* **2016**, *6* (1), 51. DOI: 10.5539/jmsr.v6n1p51
- [122] Rösch, P.; Schmidt, H.; Bruder, T., A novel approach to simulate the stiffness behaviour of spot welded vehicle

- structures under multi axial variable amplitude loading. *MATEC Web of Conferences* **2018**, 165. DOI: 10.1051/mateconf/201816517005
- [123] Li, S.; Feng, X., Study of structural optimization design on a certain vehicle body-in-white based on static performance and modal analysis. *Mechanical Systems and Signal Processing* **2020**, 135. DOI: 10.1016/j.ymssp.2019.106405
- [124] Ryberg, A. B.; Nilsson, L., Spot weld reduction methods for automotive structures. *Structural and Multidisciplinary Optimization* **2016**, 53 (4), 923-934. DOI: 10.1007/s00158-015-1355-4